The Vacuolar Manganese Transporter MTP8 Determines Tolerance to Iron Deficiency-Induced Chlorosis in Arabidopsis[1][OPEN]

Seckin Eroglu, Bastian Meier, Nicolaus von Wirén, and Edgar Peiter*

Leibniz-Institute for Plant Genetics and Crop Plant Research, D–06466 Gatersleben, Germany (S.E., N.v.W.); and Plant Nutrition Laboratory, Institute of Agricultural and Nutritional Sciences, Faculty of Natural Sciences III, Martin Luther University Halle-Wittenberg, D–06099 Halle (Saale), Germany (B.M., E.P.)

ORCID IDs: 0000-0002-9494-7080 (S.E.); 0000-0003-3270-5825 (B.M.); 0000-0002-4966-425X (N.v.W.); 0000-0002-9104-3238 (E.P.).

Iron (Fe) deficiency is a widespread nutritional disorder on calcareous soils. To identify genes involved in the Fe deficiency response, Arabidopsis (*Arabidopsis thaliana*) transfer DNA insertion lines were screened on a high-pH medium with low Fe availability. This approach identified METAL TOLERANCE PROTEIN8 (MTP8), a member of the Cation Diffusion Facilitator family, as a critical determinant for the tolerance to Fe deficiency-induced chlorosis, also on soil substrate. Subcellular localization to the tonoplast, complementation of a manganese (Mn)-sensitive *Saccharomyces cerevisiae* yeast strain, and Mn sensitivity of *mtp8* knockout mutants characterized the protein as a vacuolar Mn transporter suitable to prevent plant cells from Mn toxicity. *MTP8* expression was strongly induced on low-Fe as well as high-Mn medium, which were both strictly dependent on the transcription factor FIT, indicating that high-Mn stress induces Fe deficiency. *mtp8* mutants were only hypersensitive to Fe deficiency when Mn was present in the medium, which further suggested an Mn-specific role of MTP8 during Fe limitation. Under those conditions, *mtp8* mutants not only translocated more Mn to the shoot than did wild-type plants but suffered in particular from critically low Fe concentrations and, hence, Fe chlorosis, although the transcriptional Fe deficiency response was up-regulated more strongly in *mtp8*. The diminished uptake of Fe from Mn-containing low-Fe medium by *mtp8* mutants was caused by an impaired ability to boost the ferric chelate reductase activity, which is an essential process in Fe acquisition. These findings provide a mechanistic explanation for the long-known interference of Mn in Fe nutrition and define the molecular processes by which plants alleviate this antagonism.

Iron (Fe) is an essential microelement for plants, finding its major role as a cofactor in redox-active proteins (Kobayashi and Nishizawa, 2012; Peiter, 2014). Although Fe is highly abundant in the earth's crust, in aerated soils, Fe forms poorly soluble hydroxides, oxides, and other inorganic precipitates, all of which are not readily available for plant uptake (Lindsay and Schwab, 1982). Consequently, the amount of Fe dissolved in the soil solution is usually far lower than that required to sustain plant growth.

For the acquisition of Fe, plants other than graminaceous species rely on the solubilization and reduction of chelated Fe(III) (Giehl et al., 2009). In Arabidopsis (*Arabidopsis thaliana*), a major contribution to Fe solubilization is made by phenolic compounds, in particular catechol-type coumarins, which act as bidentate or tridentate metal chelators and are released by roots of Fe-deficient plants (Schmid et al., 2014). Although some coumarins have the additional ability to reduce Fe(III) (Schmid et al., 2014), Fe is primarily reduced by the activity of a membrane-bound reductase (FRO2 in Arabidopsis) that transfers electrons from cytosolic NADH to apoplastic Fe(III) chelates (Yi and Guerinot, 1996; Robinson et al., 1999). This enzymatic reduction process is facilitated by an acidification of the apoplast, which is mediated by an increased activity of plasma membrane-localized P-type H^+-ATPases, such as AHA2 in Arabidopsis (Santi and Schmidt, 2009). On alkaline soils, H^+ extrusion is often insufficient to decrease the apoplastic pH. Hence, the activity of the ferric chelate reductase remains at a low, insufficient level, favoring Fe deficiency-induced chlorosis.

After reduction, divalent Fe^{2+} is taken up into epidermal and cortical cells of the root by membrane transporters of the ZRT, IRT-LIKE PROTEIN (ZIP) family. For this reason, Fe(III) reduction is a prerequisite for Fe^{2+} uptake. In Arabidopsis, the primary Fe

[1] This work was supported by the Deutsche Forschungsgemeinschaft (grant no. DFG PE1500/3–1 to E.P.), the Ministerium für Landwirtschaft und Umwelt des Landes Sachsen-Anhalt (to E.P.), and the Bundesministerium für Bildung und Forschung, Germany (grant no. FKZ 0315458B to N.v.W.).

* Address correspondence to edgar.peiter@landw.uni-halle.de.

The authors responsible for distribution of materials integral to the findings presented in this article in accordance with the policy described in the Instructions for Authors (www.plantphysiol.org) are: Nicolaus von Wirén (vonwiren@ipk-gatersleben.de) and Edgar Peiter (edgar.peiter@landw.uni-halle.de).

S.E., B.M., N.v.W., and E.P. designed research and analyzed data; S.E. and B.M. performed research; S.E., B.M., N.v.W., and E.P. wrote the article.

[OPEN] Articles can be viewed without a subscription.
www.plantphysiol.org/cgi/doi/10.1104/pp.15.01194

 © 2016 American Society of Plant Biologists. All Rights Reserved.

deficiency-inducible high-affinity Fe^{2+} importer is encoded by the *IRON-REGULATED TRANSPORTER1* (*IRT1*) gene (Eide et al., 1996; Vert et al., 2002). The expression of both *IRT1* and *FRO2* is strongly induced upon Fe deficiency. This response is controlled by the basic helix-loop-helix (bHLH)-type transcription factor FIT and further interacting bHLH proteins (Colangelo and Guerinot, 2004; Jakoby et al., 2004). In parallel to this transcriptional network that primarily regulates Fe acquisition, another regulon operates mainly in stelar tissues, which involves the bHLH transcription factor POPEYE (PYE; Long et al., 2010).

Recent work has shown that IRT1 is under extensive posttranslational control, which is essential to avoid Fe overaccumulation and toxicity. Localization analyses showed that IRT1 cycles from the trans-Golgi network/early endosomes to the plasma membrane to mediate Fe uptake or to the vacuole for degradation (Barberon et al., 2011). Interestingly, the endocytosis of IRT1 is triggered by zinc (Zn), cobalt (Co), and manganese (Mn). This may serve to limit the influx of those metals (Barberon et al., 2014). Correct trafficking of IRT1 to the plasma membrane requires the endosomal regulatory protein SNX1 (Ivanov et al., 2014). In addition, IRT1 has been shown to be ubiquitinated for degradation by a RING E3 ubiquitin ligase, IDF1 (Shin et al., 2013). The multilevel transcriptional and posttranslational control of IRT1 demonstrates the potential complexity in the regulation of Fe acquisition proteins. The mechanisms of posttranscriptional regulation of other proteins involved in Fe acquisition have not yet been studied in this depth.

A major reason for the heavy metal-dependent posttranslational regulation of the IRT1 transporter is found in its low selectivity for Fe^{2+}. Since IRT1 also permeates other divalent metals, such as Zn^{2+}, Cu^{2+}, Co^{2+}, Ni^{2+}, and Mn^{2+} (Korshunova et al., 1999; Vert et al., 2002; Schaaf et al., 2006), Fe-deficient plants risk accumulating potentially toxic amounts of those ions. The detoxification of excess Zn, nickel (Ni), and Co in Fe-deficient plants is mediated by sequestration into vacuoles, mainly of root epidermal and cortical cells, by means of CATION DIFFUSION FACILITATOR (CDF)- or IRON-REGULATED GENE (IREG)-type transporters (Arrivault et al., 2006; Schaaf et al., 2006). The compartmentalization of heavy metals into the vacuole of root cells also prevents their excessive translocation to the shoot. Among the metals overaccumulating in Fe-deficient plants, Mn has been known for a long time to exert a negative effect on Fe nutrition (Twyman, 1946), and for field-grown plants, high Mn availability is one of the major factors that induce Fe deficiency chlorosis (Lindner and Harley, 1944). Despite this fact, the molecular basis of the antagonistic Fe-Mn interaction and the mechanism by which Mn is detoxified in Fe-deficient plants have remained unclear.

To unravel new components of the Fe deficiency response of Arabidopsis, we carried out a forward genetic screen employing a collection of transfer DNA (T-DNA) insertion lines affected in the expression of Fe-regulated genes. For this purpose, we developed an agar medium with low Fe availability, rather than low total Fe concentration, to mimic the situation in calcareous soil. In this screen, we identified two lines that showed severe chlorosis. In both lines, the *METAL TOLERANCE PROTEIN8* (*MTP8*) gene, a member of the CDF family, was knocked out. In line with previously characterized MTP8 orthologs, subcellular localization and yeast complementation characterized the protein as a vacuolar Mn transporter suitable to prevent plant cells from Mn toxicity. However, our investigations revealed a crucial role of this protein in the Fe acquisition machinery, thereby safeguarding an efficient acquisition and translocation of Fe to aboveground plant parts. We further identified ferric chelate reduction as the Mn-sensitive process in the Fe deficiency response. These findings provide a mechanistic insight into the long-known interference of Mn in Fe acquisition and define the molecular process by which plants alleviate this antagonism. The general relevance of this mechanism is underlined by the hypersensitivity of *mtp8* mutants to Fe deficiency chlorosis also on calcareous soil.

RESULTS

Establishment of Growth Conditions to Screen for Defects in Fe Nutrition

In calcareous and alkaline soils, plants do not face the problem of a low total Fe amount in the soil but rather of a low solubility of soil Fe. For this reason, we developed an agar medium with elevated pH and low Fe availability to screen a collection of T-DNA insertion lines for exacerbated symptoms of Fe deficiency-induced chlorosis. The screening medium was based on one-half-strength Murashige and Skoog (MS) medium (Murashige and Skoog, 1962) containing 40 μM Mn and reduced amounts of Fe(III)-EDTA as Fe source. Plants developed chlorosis if the medium was buffered at pH 6.7 with 10 mM MES, indicating that Fe availability was limiting plant growth. Among the Fe concentrations tested, 28 μM Fe(III)-EDTA turned out to induce a mild but persisting chlorosis in young leaves of wild-type plants (Supplemental Fig. S1A). On this medium, hereafter called Fe28/Mn40, Columbia-0 (Col-0) seedlings grew in a slightly chlorotic state for more than 2 weeks, while raising the Fe concentration to 100 μM prevented the development of chlorosis (Supplemental Fig. S1A). The suitability of these growth conditions to screen for genes involved in Fe acquisition was confirmed by comparing the growth of previously characterized mutant lines. Indeed, mutants affected in Fe reduction (*fro2*; Robinson et al., 1999), Fe uptake (*irt1*; Vert et al., 2002), or Fe translocation to the shoot (*frd3*; Delhaize, 1996) all turned severely chlorotic on Fe28/Mn40, while the *pye* mutant, which is defective in Fe-dependent regulation of gene expression in inner root cells (Long et al., 2010), rather showed suppressed growth and weaker chlorosis (Supplemental Fig. S1B).

Arabidopsis *mtp8* Knockout Mutants Are Highly Susceptible to Fe Deficiency-Induced Chlorosis

A collection of T-DNA insertion lines was screened on the Fe28/Mn40 medium for hypersensitivity to low

Fe availability. The population consisted of homozygous T-DNA lines from the SALK, SAIL, and GABI collections carrying insertions in genes known to be up-regulated under Fe deficiency in a FIT- or PYE-dependent manner (Supplemental Table S1). In this screen, we identified two lines that carried a T-DNA insertion in *MTP8* (At3g58060), a gene that had not yet been associated with Fe deficiency-induced chlorosis (Fig. 1A). In one mutant line of the SALK collection, SALK_068494, a T-DNA was inserted in the first of the seven exons of the *MTP8* gene (Supplemental Fig. S2A). We named this line *mtp8-1*. In *mtp8-2* (i.e. SALK_140266), a T-DNA was inserted in the sixth exon. Reverse transcription (RT)-PCR analysis using RNA from mutant and wild-type plants revealed the loss of *MTP8* full-length transcripts in *mtp8-1* and *mtp8-2* (Supplemental Fig. S2B). Buffering of the medium to pH 6.7 was essential to identify this mutant, as the chlorotic phenotype was not apparent on Fe28/Mn40 medium at pH 5.5 (Fig. 1A). In addition, both *mtp8* mutants were indistinguishable from wild-type plants on Fe100/Mn40 medium (Fig. 1B). The chlorotic phenotype of the mutants on Fe28/Mn40 medium could also be reverted by spraying with 100 μM Fe(III)-EDTA, indicating that the mutants were susceptible to Fe deficiency and not to the lack or the toxicity of another element (Fig. 1B). When grown on a calcareous potting substrate, seedlings of the *mtp8-1* mutant were smaller and extremely chlorotic (Fig. 1C). This demonstrated that the mutant phenotype was not limited to our screening conditions on agar but was also highly relevant for growth on soil.

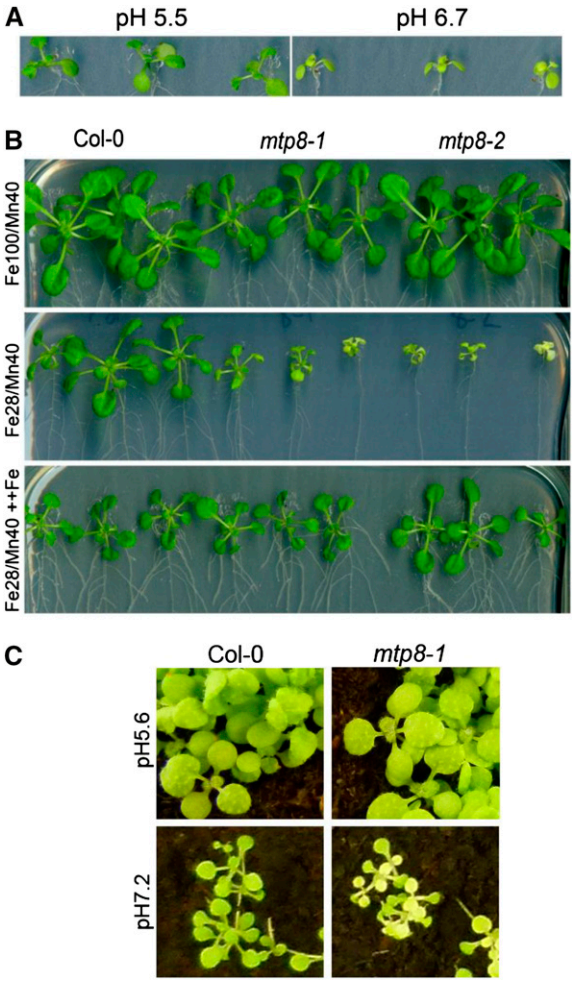

Figure 1. Two Arabidopsis T-DNA insertion lines for *MTP8*, *mtp8-1* and *mtp8-2*, are less tolerant to elevated pH-induced low Fe availability. A, Growth of wild-type seedlings on Fe28/Mn40 medium buffered to pH 6.7 or 5.5. Seedlings were cultivated for 12 d. B, Growth of *mtp8-1* and *mtp8-2* mutants on Fe100/Mn40, Fe28/Mn40, or Fe28/Mn40 with foliar application of Fe. Seedlings were cultivated for 23 d. In the foliar application treatment, a solution containing 100 μM NaFe(III)-EDTA was sprayed onto the seedlings after 9 d of cultivation on Fe28/Mn40 medium. C, Growth of the *mtp8-1* mutant on nonlimed (pH 5.6) and limed (pH 7.2) potting soil, watered with 160 μM $MnCl_2$. Plants were photographed after 19 d of cultivation.

Arabidopsis MTP8 Is Localized to the Tonoplast

Arabidopsis MTP8 belongs to the CDF family of cation transporters (Montanini et al., 2007). The most closely related characterized member of the family is ShMTP8, a vacuolar Mn transporter thought to be responsible for the high tolerance of *Stylosanthes hamata* to excess Mn (Delhaize et al., 2003). To our knowledge, Fe deficiency-related phenotypes have not been reported yet for ShMTP8 or any other plant CDF protein. To elucidate the mechanism responsible for the Fe chlorosis phenotype of the Arabidopsis *mtp8* mutants, we first determined the subcellular localization of the protein by enhanced yellow fluorescent protein (EYFP) fusion. To this end, Arabidopsis protoplasts were transformed with an *MTP8:EYFP* construct and fluorescence was observed by confocal microscopy. Fluorescence emitted by MTP8:EYFP was visible solely at the tonoplast (Fig. 2), indicating that Arabidopsis MTP8 has the same subcellular localization as ShMTP8 (Delhaize et al., 2003).

Arabidopsis *MTP8* Complements an Mn-Sensitive Yeast Strain and Transports Mn

Since ShMTP8 and Arabidopsis MTP8 share a high degree of sequence similarity, including an amino acid signature specific for the Mn subgroup of CDFs (Montanini et al., 2007), and since both are localized to the tonoplast, we hypothesized that Arabidopsis MTP8 functions in sequestering Mn ions into the vacuole and that this function is related to the Fe-deficient phenotype of the mutant. Therefore, we determined the metal selectivity of the transporter by expressing the *MTP8* complementary DNA (cDNA) in metal-hypersensitive yeast strains. Growth of yeast mutants sensitive to Co (*cot1Δ*), Zn (*zrc1Δ*), and copper (*cup2Δ*) on medium containing high concentrations of the respective metals was not improved by the expression of *MTP8* (Fig. 3A). In contrast, growth of the Mn-hypersensitive mutant *pmr1Δ* at elevated Mn concentrations was considerably

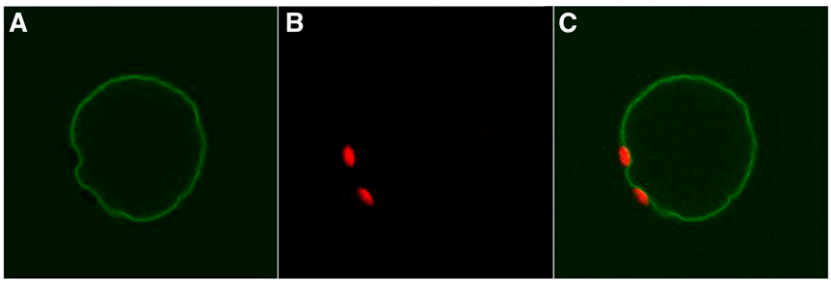

Figure 2. Arabidopsis MTP8:EYFP localizes to the tonoplast. Mesophyll protoplasts of Arabidopsis Col-0 were transformed with an *MTP8:EYFP* construct. Fluorescence was observed 24 h after transformation. A, MTP8:EYFP fluorescence. B, Chlorophyll autofluorescence. C, Merged image of A and B.

improved when transformed with *MTP8*. *PMR1* encodes a calcium/Mn-ATPase that confers Mn tolerance to yeast (Antebi and Fink, 1992). The *MTP8*-expressing *pmr1Δ* mutant grew well even on medium containing Mn concentrations that were strongly inhibitory to the wild type. Mn transport activity of MTP8 was further supported by direct transport assays on microsomal vesicles. Vesicles of *MTP8*-expressing *pmr1Δ* yeast accumulated $^{54}Mn^{2+}$ within a short time frame, whereas the empty vector-transformed strain did not show transport activity (Fig. 3B). These observations indicated that Arabidopsis MTP8, like ShMTP8, transports Mn into the vacuole.

The Arabidopsis *mtp8-1* Mutant Is Moderately Hypersensitive to High Mn

To test whether Arabidopsis MTP8 confers tolerance to excess Mn, wild-type and *mtp8-1* mutant seedlings were subjected to increasing concentrations of the metal. At elevated Mn supply, root growth rates were repressed more strongly in the *mtp8-1* mutant than in the wild type (Fig. 4, A and B; Supplemental Fig. S3). After 2 weeks of growth on elevated Mn concentrations, the shoot fresh weight of the mutant seedlings was also moderately, but significantly, lower than that of the wild type (Fig. 4, A and C). Since the repression of primary root growth is a typical Mn toxicity symptom (Peiter et al., 2007), this observation indicated that MTP8 indeed increases the tolerance of Arabidopsis to excess Mn.

Overexpression of Arabidopsis *MTP8* Increases Mn Sequestration in Root Vacuoles

To further examine the function of MTP8 in Mn transport, overexpression lines were generated in which the expression of *MTP8* is driven by the cauliflower mosaic virus (CaMV) 35S promoter. Quantitative RT-PCR analysis showed that expression of the *MTP8* gene was strongly increased in these lines (Fig. 5A). The lines 35S:MTP8#OE2 and 35S:MTP8#OE4, which had approximately 7,000- and 3,000-fold increased *MTP8*

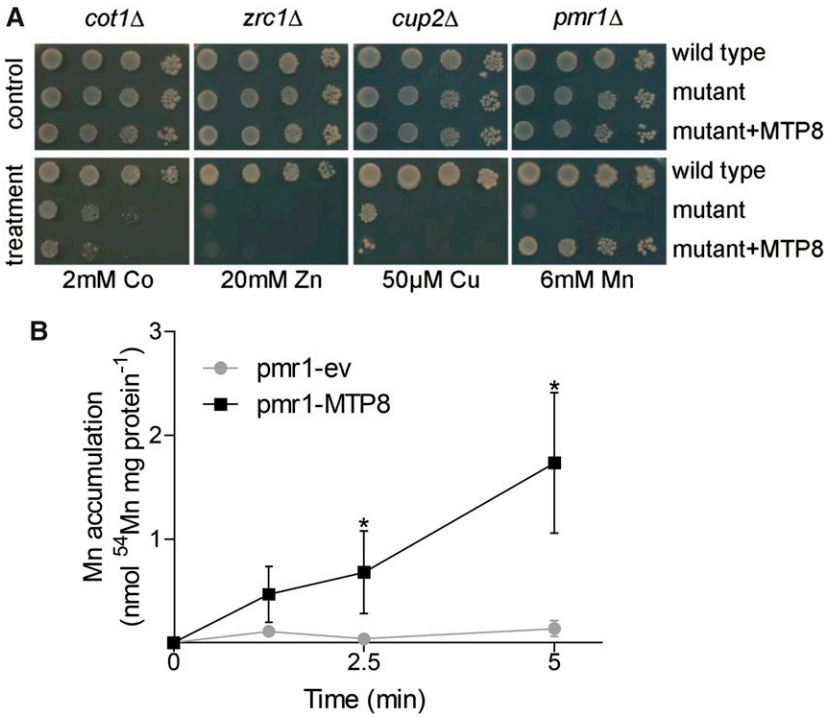

Figure 3. Arabidopsis *MTP8* complements an Mn-sensitive yeast strain, but not yeast strains sensitive to Zn, Co, or copper (Cu), and mediates Mn transport. A, Cultures of yeast strains sensitive to Co (*cot1Δ*), Zn (*zrc1Δ*), Cu (*cup2Δ*), and Mn (*pmr1Δ*) were serially diluted and dropped onto plates containing the indicated concentrations of the respective metals. B, Microsomal membrane vesicles from *pmr1Δ* yeast transformed with pFL61 (circles) or pFL61:MTP8 (squares) were analyzed for $^{54}Mn^{2+}$ uptake activity. Vesicles were incubated in uptake buffer containing 100 μM Mn, and aliquots (50 μg of protein) were separated from the medium by vacuum filtration at the indicated time points. Values in the absence of ATP were subtracted to correct for unspecific adsorption. Data are means ± SD of three independent uptake experiments conducted on different microsomal preparations. Asterisks indicate that the mean of the pFL61:MTP8 strain is significantly different from the mean of the pFL61 strain according to Student's *t* test ($P < 0.05$).

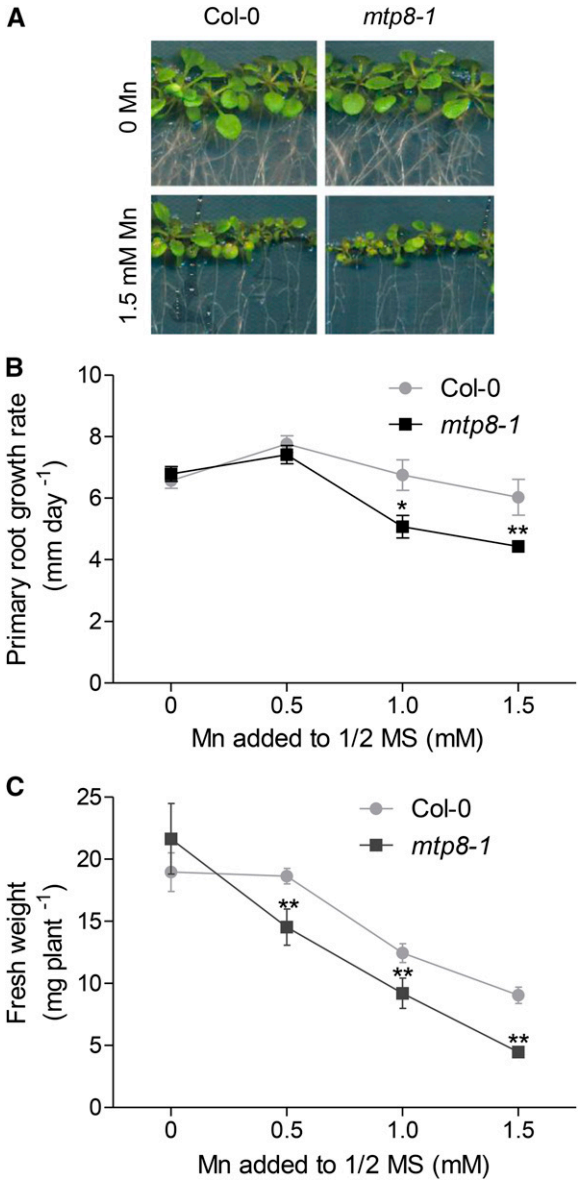

Figure 4. Arabidopsis *MTP8* is required for tolerance to high Mn concentrations. A, Growth of wild-type and *mtp8-1* seedlings on one-half-strength MS agar supplemented with no or 1.5 mM $MnSO_4$. Seedlings were cultivated for 14 d. B, Primary root growth rates of Col-0 (circles) and *mtp8-1* (squares) seedlings on one-half-strength MS medium supplemented with increasing amounts of Mn. Each data point is the mean ± SD of the linear regression of the root lengths of 16 seedlings determined as shown in Supplemental Figure S3. C, Effects of Mn on shoot fresh weight of 14-d-old wild-type (circles) and *mtp8-1* (squares) seedlings. Data are means ± SD of 16 seedlings per line. Asterisks indicate that the mean of the *mtp8-1* line is significantly different from the mean of Col-0 according to Student's *t* test (*, $P < 0.05$ and **, $P < 0.01$). All data are derived from the same experiment. The experiment was repeated twice with similar results.

transcript levels, respectively, were selected for further experiments. On one-half-strength MS medium (pH 5.5) supplemented with 200 μM Mn, both overexpressors accumulated significantly higher Mn levels in the roots than the wild type (Fig. 5B), indicating that an overexpression of *MTP8* increases Mn sequestration primarily in roots. In contrast, root Fe concentrations did not differ between the genotypes, while shoots of the overexpressors contained slightly lower Fe concentrations than the wild type. Elemental analyses of isolated root vacuoles of plants grown under the same conditions indicated that vacuolar sequestration of Mn was indeed increased in the overexpressors, whereas Fe concentrations were not altered (Fig. 5C). Taken together, these data supported the notion that vacuolar Mn sequestration by MTP8 in roots is involved in controlling the long-distance translocation of Mn from roots to shoots.

Arabidopsis *MTP8* Is Transcriptionally Up-Regulated on High-Mn Medium in a FIT-Dependent Manner

In order to investigate if *MTP8* is transcriptionally regulated by Mn, we analyzed its expression in seedlings subjected to increasing Mn concentrations. In roots, *MTP8* expression was induced 8- or 12-fold when plants were cultivated on medium supplemented with 1.5 or 2 mM Mn, respectively (Fig. 6A). This confirmed an Mn-dependent transcriptional control of *MTP8*.

Based on a transcriptome analysis of the Arabidopsis *fit* mutant, *MTP8* has been reported to be up-regulated under Fe deficiency by the transcription factor FIT (Colangelo and Guerinot, 2004). In order to confirm this finding, wild-type and *fit* mutant plants precultured on one-half-strength MS medium were transferred either to the same Fe-sufficient medium or to Fe-depleted medium (one-half-strength MS medium without Fe and containing 100 μM ferrozine). After 5 d of cultivation, *MTP8* expression in Fe-sufficient roots was low in both wild-type and *fit* mutant plants (Fig. 6B). As expected, *MTP8* expression in the wild type was induced approximately 50-fold under Fe deficiency. In contrast, *MTP8* transcript levels remained unaltered in the Fe-deficient *fit* mutant. This result confirmed that, under Fe deficiency, *MTP8* is up-regulated in a FIT-dependent manner.

In order to determine whether the increased expression of *MTP8* under high-Mn stress was also dependent on FIT, wild-type and *fit* mutant plants precultured on one-half-strength MS medium were transferred either to the same medium or to one-half-strength MS medium supplemented with 2 mM Mn. After 5 d on basal one-half-strength MS medium, the expression of *MTP8* was similar in wild-type and *fit* mutant plants (Fig. 6C). Supplementation of the medium with 2 mM Mn caused a 10-fold increase of *MTP8* expression in the wild type, whereas *MTP8* transcript abundance did not change in the *fit* mutant. This indicated that the transcriptional up-regulation of *MTP8* under high Mn is mediated by FIT.

In Fe-deficient plants, *FIT* itself is also transcriptionally up-regulated (Colangelo and Guerinot, 2004; Buckhout et al., 2009). To examine if this is also the case under high-Mn stress, we determined its expression in the samples in which *MTP8* expression had been analyzed (Fig. 6A). Like *MTP8*, *FIT* expression was induced when plants were cultivated on medium supplemented

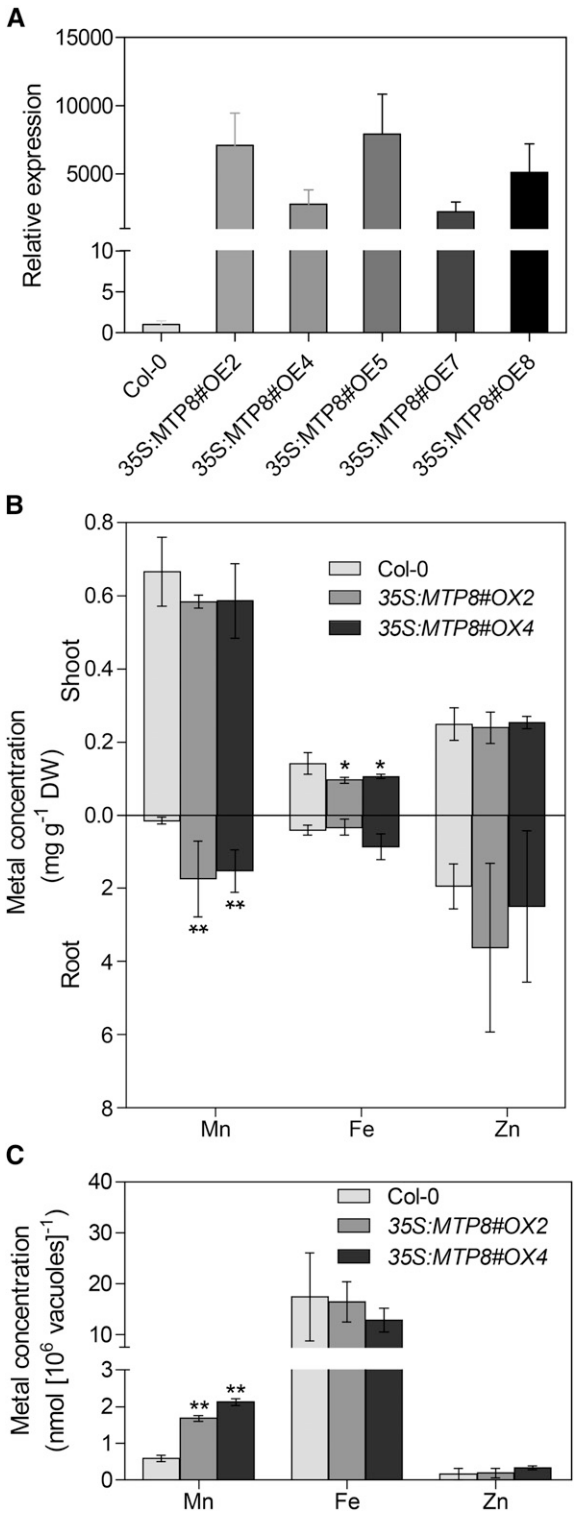

Figure 5. Arabidopsis *MTP8* overexpressor lines accumulate more Mn in the roots and sequestrate more Mn in root vacuoles than wild-type plants. A, Expression of *MTP8* in 35S:MTP8 lines. Seedlings were grown on one-half-strength MS medium for 14 d. Expression of *MTP8* was determined by quantitative RT-PCR. Data represent means ± SD of three samples. B, Mn, Fe, and Zn concentrations of *MTP8* overexpressors grown on one-half-strength MS agar medium (pH 5.5) containing 240 μM Mn. Seedlings of Col-0 (light gray), 35S:MTP8#OE2 (medium gray), and 35S:MTP8#OE4 (dark gray) were cultivated for 12 d. Shoots and roots were separated, and Mn, Fe, and Zn concentrations were determined by inductively coupled plasma-optical emission spectroscopy (ICP-OES). Data are from four replicate pools, each consisting of four seedlings obtained from different plates. DW, Dry weight. C, Mn and Fe contents in root vacuoles. Vacuoles were isolated from roots of 8-week-old plants growing in nutrient solution containing 240 μM Mn and analyzed by inductively coupled plasma-mass spectrometry (ICP-MS). Data are means from three plants. Asterisks indicate that the mean of the overexpressor line is significantly different from the mean of the Col-0 line according to Student's *t* test (*, $P < 0.05$ and **, $P < 0.01$). Error bars represent SD. The experiments were repeated twice with similar results.

with 1.5 or 2 mM Mn (Fig. 6A). In addition to *FIT*, the expression of the *FIT*-regulated genes *IRT1* and *FRO2* was also increased in high-Mn-stressed plants (Fig. 6A). Similar trends in the expression of *FIT*, *IRT1*, *FRO2*, and *MTP8* underlined that the induction of *MTP8* by Mn stress is FIT dependent and that high Mn concentrations in the medium trigger Fe deficiency responses.

The Arabidopsis *MTP8* Promoter Is Active in the Outer Cell Layers of Fe-Deficient Roots

PromoterMTP8:*GUS* lines were generated to characterize the expression pattern of *MTP8*. To confirm that the gene was induced under Fe deficiency, 10-d-old seedlings were transferred from one-half-strength MS medium to either the same medium or to Fe-free one-half-strength MS medium supplemented with 100 μM ferrozine, cultivated further for 2 d, and stained for GUS activity. After 2 h of incubation in GUS staining solution, the Fe-deficient roots, but not the Fe-sufficient ones, showed an intense blue staining (Fig. 7A). GUS activity was evident along the entire root except for the meristematic regions and the oldest parts of the main root. Cross sections of the root revealed that only epidermis, root hairs, and cortex were stained, demonstrating that *MTP8* expression in the root is limited to the outer cell layers (Fig. 7B). After an overnight incubation of the shoot, only cotyledons were weakly stained (Fig. 7C), and staining intensity was not altered under Fe deficiency (data not shown). The staining in the cotyledons was less intense than in the root, although the shoot was incubated much longer in GUS staining solution, indicating that *MTP8* expression was confined predominantly to roots subjected to Fe deficiency. This was confirmed with *PromoterMTP8*:*MTP8*:*EYFP* lines, which showed fluorescence in the outer cell layers of the root only if subjected to Fe deficiency (Fig. 7, D and E).

Iron Deficiency-Induced Chlorosis in *mtp8* Knockout Mutants Is Alleviated by Decreasing Mn Concentrations

Arabidopsis *mtp8* mutants showed severe chlorosis on Fe-limiting medium (Fig. 1), *MTP8* is regulated by

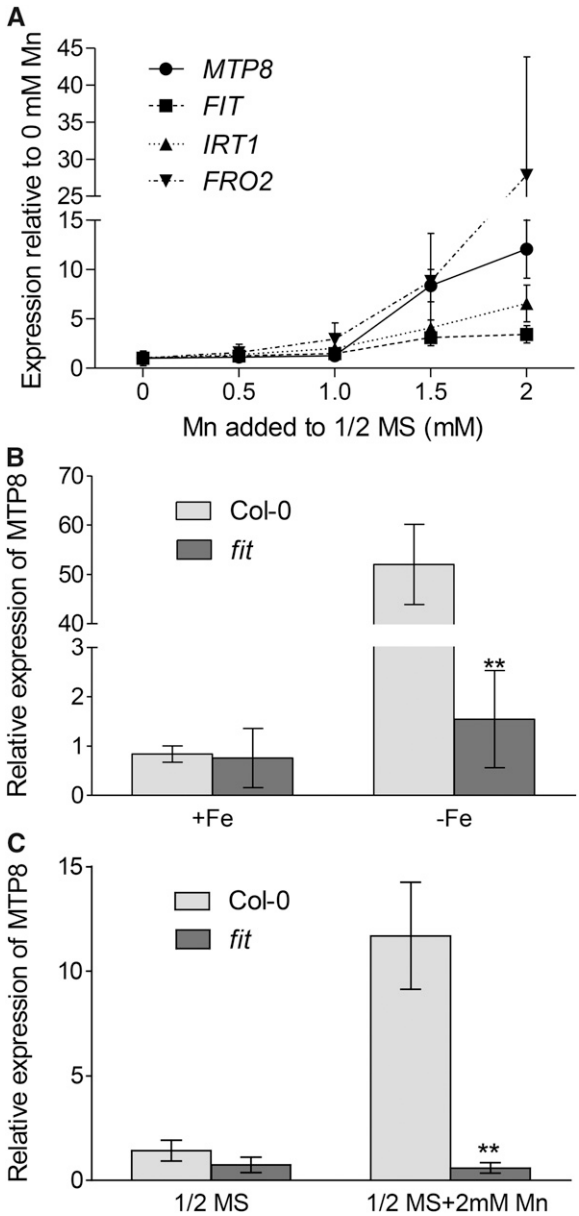

Figure 6. Expression of Arabidopsis *MTP8* is up-regulated on high-Mn medium and low-Fe medium in a FIT-dependent manner. A, Effects of high Mn on the expression of *MTP8* (circles), *FIT* (squares), *IRT1* (triangles), and *FRO2* (inverted triangles) in roots. Seedlings were grown for 21 d on near-vertical one-half-strength MS plates supplemented with $MnSO_4$ as indicated. Expression levels were normalized to *ACTIN2* and calculated relative to the expression level on control plates (0 Mn). Data represent means ± SD of four plates per Mn concentration, with each plate containing 20 plants. The experiment was repeated twice with similar results. B, FIT dependence of *MTP8* expression on low-Fe medium. Col-0 (light gray) and *fit* (dark gray) seedlings were cultivated on one-half-strength MS agar medium for 10 d and transferred to either fresh one-half-strength MS medium (+Fe) or Fe-free one-half-strength MS medium supplemented with 100 μM ferrozine (−Fe). Roots were harvested after 5 d of treatment. Data are means ± SD of four samples, each consisting of five plants. C, FIT dependence of *MTP8* expression on high-Mn medium. Col-0 (light gray) and *fit* (dark gray) seedlings were cultivated on one-half-strength MS agar medium for 10 d and transferred to either fresh one-half-strength MS medium or one-half-strength MS medium supplemented with 2 mM Mn. Roots were harvested after 5 d of treatment. Data are means ± SD of four samples, each consisting of five plants. Asterisks indicate that the mean of the *fit* line is significantly different from the mean of the Col-0 line according to Student's *t* test (**, $P<0.01$).

FIT (Fig. 6), and MTP8 plays a role in Mn tolerance (Fig. 4). Therefore, we hypothesized that the MTP8-dependent chlorosis observed on medium with low Fe availability is related to a disturbed Mn homeostasis. To assess the effect of Mn supply, plants were precultured on Fe28/Mn0 (Fe28 devoid of Mn) for 1 week, transferred to the same medium or to Fe28/Mn40 or Fe28/Mn160, and cultivated further for 1 week. On Fe28/Mn40, *mtp8* mutants became chlorotic, as observed before, which was also reflected in a decreased chlorophyll concentration (Fig. 8). Shoot fresh weight of the mutants was lower than that of the wild type, whereas primary root length did not differ significantly in *mtp8-1* and was only slightly shorter in *mtp8-2* (Fig. 8).

In contrast to the plants on Fe28/Mn40 medium, mutants transferred to medium not supplemented with Mn (Fe28/Mn0) neither showed chlorosis symptoms nor differed from the wild type in chlorophyll concentration, shoot fresh weight, or primary root length (Fig. 8). On the other hand, increasing the medium Mn concentration 4 times (Fe28/Mn160) induced an extensive chlorosis on newly emerging leaves, resulting in low chlorophyll concentrations in the *mtp8* mutant lines as well as in the wild type. Besides a decreased shoot fresh weight, both mutants now also showed a strong repression of primary root growth, which indicated primary Mn toxicity at this elevated Mn supply (Fig. 8).

Based on this experiment, we concluded that the Fe deficiency phenotype of *mtp8* mutants depends strongly on the medium concentration of Mn. Furthermore, the Mn-induced exacerbation of chlorosis in the wild type growing on Fe-limiting medium clearly underlined the antagonistic relationship between Fe and Mn.

Arabidopsis *mtp8* Mutants Are Altered in Mn and Fe Translocation

Since the increased vulnerability of the *mtp8* mutants to Fe deficiency depended on the Mn concentration in the medium (Fig. 8), we determined the concentration and distribution of both elements in plants grown at different Fe and Mn levels. Plants were precultured for 1 week either on (1) Fe100/Mn0 and transferred to the same medium or to Fe100/Mn40 or on (2) Fe28/Mn0 and transferred to either the same medium or to Fe28/Mn40. Fe and Mn concentrations in roots and shoots were determined after 1 week of treatment. As shown in Figure 9, on medium not supplemented with Mn, wild-type and mutant plants did not differ in their Fe, Mn, and Zn concentrations at sufficient or low Fe supply. In contrast, when Mn was included in the low- or

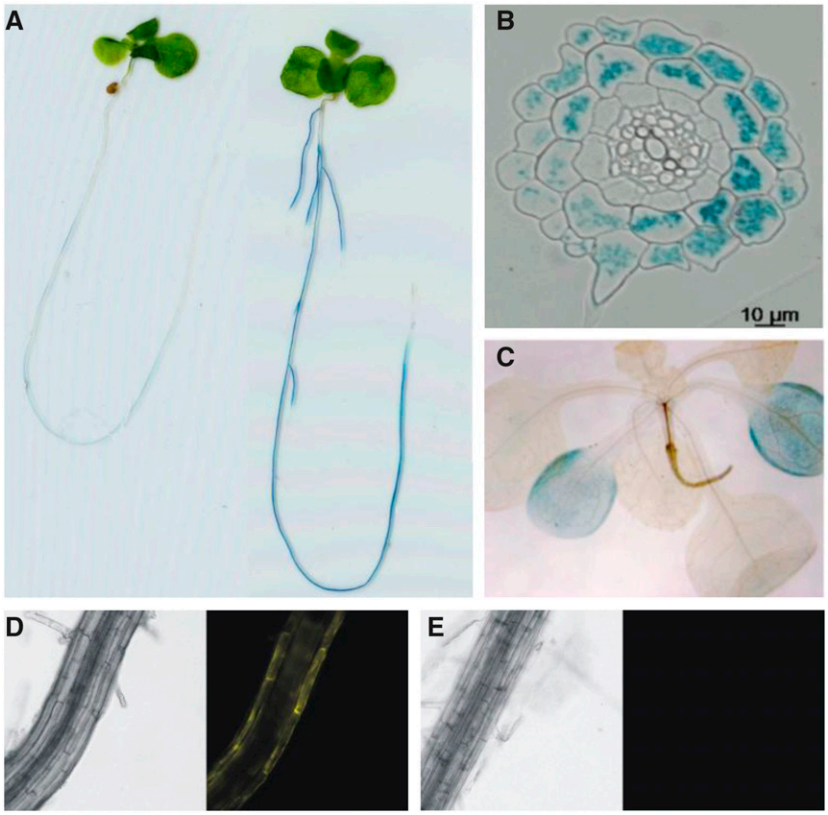

Figure 7. Activity of the Arabidopsis *MTP8* promoter in roots is restricted to outer cell layers and strongly activated upon Fe deficiency. Col-0 plants transformed with a *promoterMTP8*:*GUS* or a *promoterMTP8*:*MTP8*:*EYFP* construct were grown on one-half-strength MS agar for 10 d, transferred to plates supplemented with 100 μM ferrozine to render Fe unavailable or to one-half-strength MS control plates, and cultivated further for 2 d. A, Staining of *promoterMTP8*:*GUS*-transformed seedlings grown on Fe-sufficient (left) or Fe-deficient (right) medium after incubation for 2 h in GUS staining solution. B, Cross section of a root from a seedling grown on Fe-deficient medium and stained as in A. C, Staining of a *promoterMTP8*:*GUS*-transformed shoot grown on Fe-deficient medium after incubation for 24 h in GUS staining solution and removal of chlorophyll. D and E, Bright-field (left) and fluorescence (right) images of the root of a *promoterMTP8*:*MTP8*:*EYFP*-transformed seedling grown on Fe-deficient (D) or Fe-sufficient (E) medium.

high-Fe medium, Mn and Fe concentrations in the mutant were highly distinct from those in the wild type. The most drastic difference was observed for the Mn concentration in the roots of plants grown on Fe28/Mn40, which was approximately 5 times higher in the wild type than in the *mtp8-1* mutant (Fig. 9), whereas the shoot Mn concentration was more elevated in the mutant. The same effect was apparent on Fe100/Mn40. Hence, when grown on Mn40 medium, the *mtp8-1* mutant not only retained less Mn in the roots than the wild type but also translocated a higher proportion of Mn to the shoot. Concentrations of Zn were not decreased but even increased in the *mtp8-1* mutant growing on Fe28/Mn40 (Fig. 9). This underlines that MTP8 specifically sequesters Mn.

In contrast to Mn, the concentration of Fe in mutant shoots grown on Fe28/Mn40 was reduced to approximately 20 μg g^{-1} dry weight (Fig. 9), which was only half of that of the wild type and far below the critical level for chlorosis-free growth of Arabidopsis (Gruber et al., 2013; Schmid et al., 2014). Across many species, it is established that plants require 50 to 150 μg g^{-1} dry weight Fe (Marschner, 2012). This result confirmed that the chlorotic phenotype of the *mtp8-1* mutant was due to Fe deficiency. Fe concentrations in mutants cultivated on high-Fe medium (Fe100/Mn40) were also lower than those in the wild type but were still in the sufficient range.

The decreased shoot Fe concentrations in the *mtp8-1* mutants growing on Mn40 medium confirmed that their chlorotic phenotype was due to Fe deficiency and indicated that Fe uptake and/or translocation were inhibited. To examine Fe translocation to the shoot, xylem exudate was collected from plants cultivated on liquid Fe28/Mn40 medium. As expected, the Fe translocation rate, as related to root dry weight, was much lower in the *mtp8-1* mutant (Supplemental Fig. S4). To determine if the diminished Fe translocation to the shoot of the mutant is due to an impaired xylem loading of Fe, we analyzed Fe accumulation in roots by Perls's staining. A mutant of the citrate transporter *FRD3*, which is defective in loading Fe into the xylem, served as a positive control. Unlike *frd3-3*, *mtp8-1* did not accumulate increased amounts of Fe in root tissues (Supplemental Fig. S5), which corresponds to the similar or lower root Fe concentrations in the *mtp8-1* mutant on Mn40 medium (Fig. 9). These results indicate that Fe acquisition, rather than xylem loading and root-to-shoot translocation, was affected in the mutant.

The Transcriptional Fe Deficiency Response Is Increased in the Presence of Mn in the *mtp8-1* Mutant

The higher susceptibility to chlorosis and the decreased Fe acquisition in the *mtp8-1* mutant in the presence of Mn could have been caused by an inhibition of the transcriptional Fe deficiency response. Therefore, we analyzed the expression of genes known to be required for Fe acquisition and to be up-regulated by Fe deficiency on Fe28 medium containing 40 μM or no Mn. In the wild type, addition of Mn to low-Fe medium led

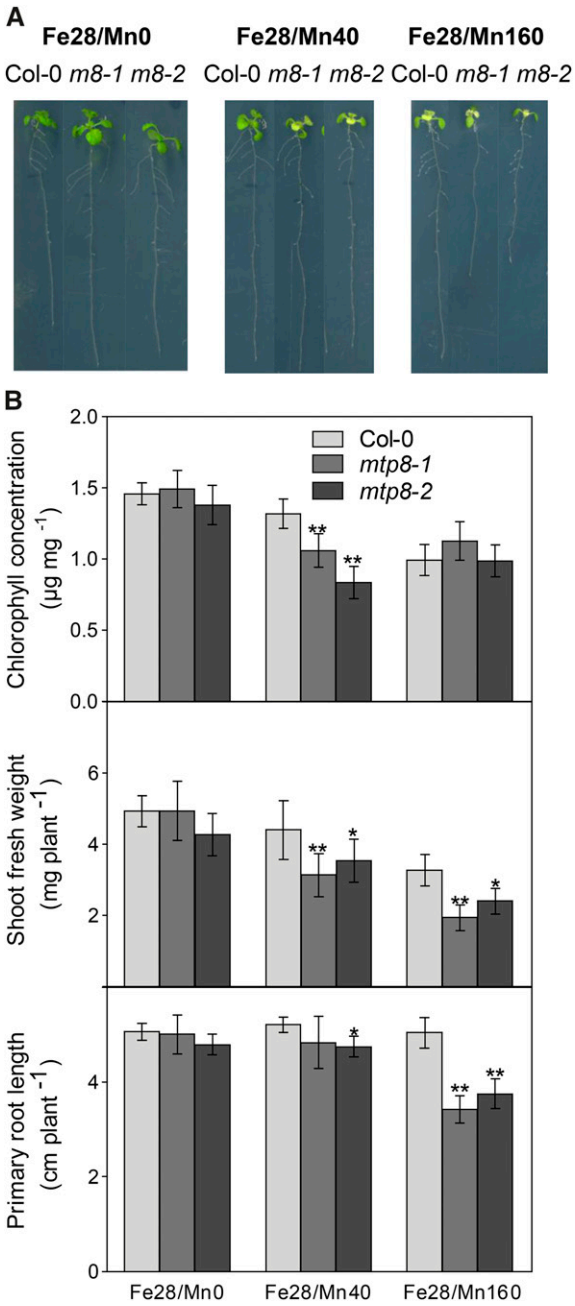

Figure 8. Arabidopsis *mtp8-1* and *mtp8-2* mutants show Fe deficiency-induced chlorosis, a repression in primary root elongation, and a decrease in shoot fresh weight if Mn is present in the medium. A, Growth of *mtp8* mutant lines grown on low-Fe medium containing different concentrations of Mn. Seedlings were precultured on Fe28/Mn0 for 1 week, transferred to Fe28/Mn0, Fe28/Mn40, or Fe28/Mn160, and cultivated further for 1 week. B, Chlorophyll concentration, shoot fresh weight, and primary root length of Col-0 (light gray), *mtp8-1* (medium gray), and *mtp8-2* (dark gray) seedlings treated as shown in A. Data are from five replicate pools, each consisting of three seedlings obtained from different plates. Asterisks indicate that the mean of the mutant line is significantly different from the mean of the Col-0 line according to Student's *t* test (*, $P < 0.05$ and **, $P < 0.01$). Error bars represent SD.

to an increased expression of the transcription factor genes *FIT*, *bHLH38*, *bHLH101*, and *MYB72*, the nicotianamine synthase gene *NAS4*, as well as the Fe acquisition genes *IRT1* and *FRO2* (Fig. 10). Paradoxically, the transcriptional response of all analyzed genes was significantly more pronounced in the *mtp8-1* knockout line. These data indicated that Mn triggers Fe deficiency responses and that a loss of *MTP8* exacerbates this antagonism, but the transcriptional response to the perceived Fe deficiency is not hampered in the mutant.

Mn Inhibits the Ferric Chelate Reductase Activity of Fe-Deficient *mtp8-1* Seedlings

To be able to analyze direct physiological responses to Fe deficiency in the presence of Mn, we attempted to avoid possible side effects arising from long-term stress. Consequently, we increased the stress intensity by decreasing Fe and increasing Mn concentrations in the medium. Seedlings were precultured on Fe14/Mn0 medium for 11 d, transferred to Fe100/Mn0, Fe0/Mn0, or Fe14/Mn320 medium, and cultivated further for 72 h. On Fe14/Mn320 medium, *mtp8-1* seedlings developed chlorotic shoots within 24 h of treatment (Fig. 11A). Hence, the development of the chlorotic phenotype was accelerated by increasing the Mn-to-Fe ratio in the medium.

Since the Fe deficiency response was induced at the transcriptional level, but the Fe concentration was not increased, in *mtp8-1* plants (Figs. 9 and 10), we reasoned that the function of a component of the Fe acquisition machinery may be impaired in the mutant. As a strategy I plant, Arabidopsis requires an inducible ferric chelate reductase to reduce Fe(III) for uptake. The activity of this enzyme is strongly increased under Fe deficiency. Accordingly, when seedlings precultured under low-Fe conditions (Fe14/Mn0) were transferred to Fe-sufficient medium (Fe100/Mn0), the ferric chelate reductase activity of mutant and wild-type seedlings decreased continuously (Fig. 11B). Conversely, on a zero-Fe medium (Fe0/Mn0), reductase activity increased strongly within the first 24 h and to the same extent in wild-type and *mtp8-1* plants. Thus, in the absence of Mn, wild-type and *mtp8-1* mutant plants did not differ in their ferric chelate reductase activities under either sufficient or deficient Fe supply.

Similar to the effect of absolute Fe limitation on Fe-free medium, the supplementation of the low-Fe medium with Mn (Fe14/Mn320) caused a 3-fold increase in ferric chelate reductase activity in the wild type within 24 h (Fig. 11B). In stark contrast, the induction of ferric chelate reductase activity on the Mn-containing low-Fe medium was far less pronounced in the *mtp8-1* mutant, although the mutant plants showed aggravating Fe deficiency symptoms under those conditions (Fig. 11A). These data indicated that Mn inhibits the ferric chelate reductase activity of the Fe-deficient *mtp8-1* mutant.

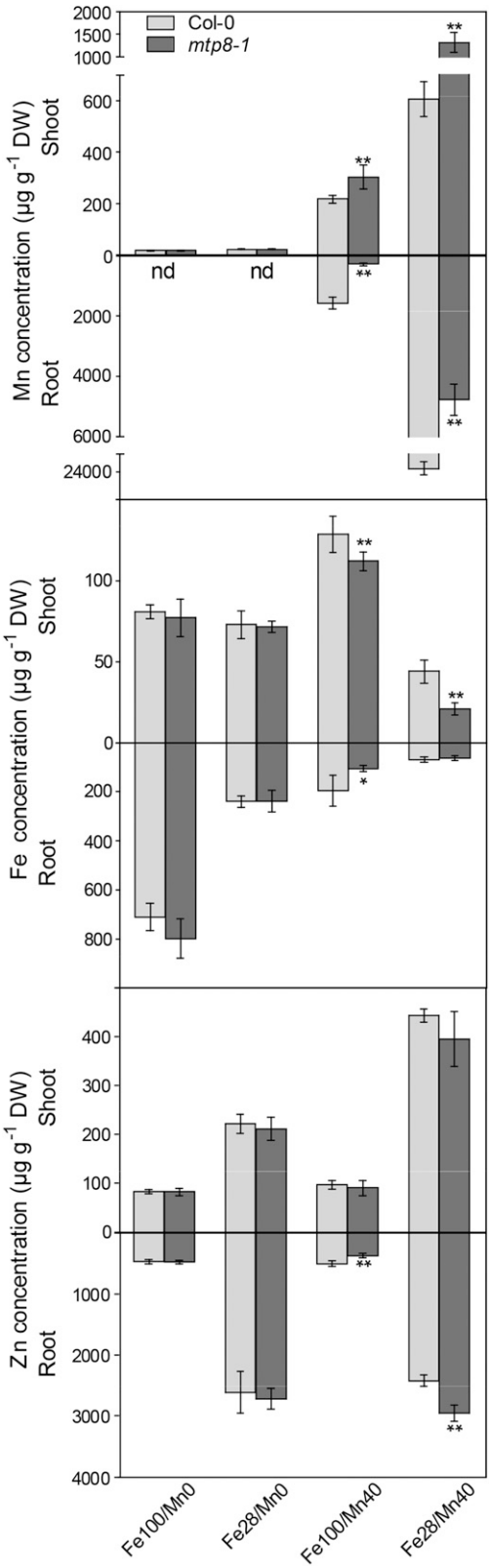

Figure 9. Arabidopsis *mtp8-1* seedlings have an increased root-to-shoot translocation of Mn and are Fe deficient on Mn-containing low-Fe medium. Seedlings of Col-0 (light gray) and *mtp8-1* (dark gray) were precultured on Fe100/Mn0, Fe28/Mn0, Fe100/Mn40, or Fe28/Mn40 agar for 1 week. Seedlings of similar size were transferred to the same media and cultivated further for 1 week. Concentrations of Mn, Fe, and Zn were determined by ICP-OES. Data are from four replicate pools, each consisting of four seedlings obtained from different plates. The experiment was conducted twice with comparable results. Asterisks indicate that the mean of the mutant line is significantly different from the mean of the Col-0 line according to Student's *t* test (*, $P < 0.05$ and **, $P < 0.01$). Error bars represent SD. nd, Not detectable.

The Fe deficiency-induced ferric chelate reductase has a low optimum pH (Susín et al., 1996). To examine if the diminished Fe(III) reduction capacity of the *mtp8-1* mutant might be caused by a decreased rhizosphere acidification, plants that were treated as in the ferric chelate reductase assay were transferred onto agar medium that contained Bromocresol Purple as a pH indicator. Surprisingly, the only roots that produced a marked yellow (i.e. acidified) rhizosphere were those of *mtp8-1* seedlings grown on Fe14/Mn320 (Supplemental Fig. S6). This observation indicated that, in contrast to ferric chelate reductase, the activity of the H^+-ATPase was up-regulated and thus reflected the aggravated Fe deficiency status of the *mtp8-1* mutant. Thus, the impaired ferric chelate reductase activity was not due to an insufficient rhizosphere acidification.

DISCUSSION

It has long been known that Fe nutrition in plants is antagonistically affected by Mn. In numerous classical studies, increased Mn availability induced Fe deficiency symptoms, irrespective of whether plants were grown in the field or on standard growth medium (Gile, 1916; Somers and Shive, 1942; Twyman, 1946; Hewitt, 1948; Sideris and Young, 1949). The negative interaction between Fe and Mn has been explained by their similar solubility characteristics in soil and by competition for uptake or translocation (Marschner, 2012). This was supported at the molecular level when IRT1 was found to permeate also Mn besides Fe (Korshunova et al., 1999; Vert et al., 2002). In our search for Arabidopsis genes involved in Fe acquisition, we identified *MTP8* as a critical determinant of Fe deficiency tolerance whenever Mn is present. Our data indicate that, in the absence of MTP8, Mn inhibits the ferric chelate reductase activity. Therefore, the physiological role of this transporter does not merely lie in the sequestration of Mn into the vacuole of root cells but primarily in securing Fe acquisition. In line with this, the regulation of MTP8 is not primarily linked with excess Mn supply but rather with the induction of the Fe acquisition machinery under low Fe availability.

Arabidopsis MTP8 Is a Vacuolar Mn Transporter in Roots

Arabidopsis MTP8 belongs to the CDF family of metal transporters. This family has 12 members in Arabidopsis, of which only a few have been characterized so far (Montanini et al., 2007; Gustin et al., 2011;

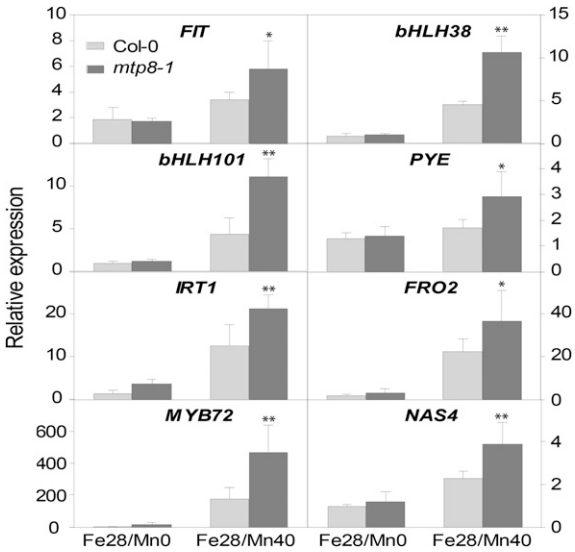

Figure 10. The transcriptional Fe deficiency response is increased in *mtp8-1* in the presence of Mn. Col-0 (light gray) and *mtp8-1* (dark gray) seedlings were cultivated for 7 d on Fe28/Mn0 or Fe28/Mn40. The expression of the Fe deficiency-responsive genes *FIT*, *bHLH38*, *bHLH101*, *PYE*, *IRT1*, *FRO2*, *MYB72*, and *NAS4* in roots was determined by quantitative RT-PCR. Data are means ± SD of four samples, each consisting of three roots obtained from different plates. Asterisks indicate that the mean of the mutant line is significantly different from the mean of the Col-0 line according to Student's *t* test (*, $P < 0.05$ and **, $P < 0.01$). The experiment was repeated three times with comparable results.

Ricachenevsky et al., 2013). An ortholog from an Mn-accumulating legume, *S. hamata*, ShMTP8 (renamed from ShMTP1 for consistency; Montanini et al., 2007), is the founding member of the Mn subgroup in the CDF family (Delhaize et al., 2003) and contains an amino acid signature that coincides with Mn specificity (Montanini et al., 2007). Our yeast complementation and direct transport assays provide experimental evidence that also Arabidopsis MTP8 has a transport activity for Mn (Fig. 3). Like ShMTP8, the Arabidopsis MTP8:EYFP fusion protein resided in the tonoplast (Fig. 2). In accord with a function of Arabidopsis MTP8 in Mn detoxification, the growth of *mtp8* mutants was impaired by high Mn (Fig. 4), and *MTP8* expression was increased under excess Mn supply (Fig. 6). Mn specificity and vacuolar localization were recently also demonstrated for MTP8 orthologs in cucumber (*Cucumis sativus*; Migocka et al., 2014) and rice (*Oryza sativa*; Chen et al., 2013). The function of MTP8 to sequester Mn into vacuoles, therefore, is widely conserved across species, with the possible exception of barley (*Hordeum vulgare*), where MTP8 homologs have been localized to the Golgi apparatus (Pedas et al., 2014). However, the circumstances under which this function is employed may differ. Interestingly, unlike the Arabidopsis and cucumber orthologs, *OsMTP8.1* from rice is expressed almost exclusively in the shoot, and shoots of an *osmtp8.1* mutant contained less Mn (Chen et al., 2013). Both findings are opposite to what we observed with Arabidopsis in this study (Figs. 7 and 9). The different functionality of MTP8 in the graminaceous species rice, as compared with the dicots Arabidopsis and cucumber, may be related to their Fe acquisition strategies and/or to the Mn availability in their natural environment. In lowland rice, reducing soil conditions often lead to a concomitant excess of Mn^{2+} and Fe^{2+} (Marschner, 2012); i.e. a situation where elevated Mn translocation to the shoot goes along with elevated Fe availability and uptake. The additional expression of *OsMTP8.1* in leaves may then increase the whole-plant capacity of rice to compartmentalize Mn in vacuoles.

Besides MTP8, MTP11 has been shown to be a major factor for the tolerance of Arabidopsis to high Mn concentrations (Peiter et al., 2007). Unlike MTP8, MTP11 is present in a compartment that colocalizes with markers for the prevacuolar compartment (Delhaize et al., 2007) and the Golgi apparatus (Peiter et al., 2007), which has recently been confirmed for an ortholog from *Beta vulgaris* (Erbasol et al., 2013). On high-Mn medium, *mtp11* mutants were much more impaired in growth than *mtp8* mutants (compare Fig. 5 and Peiter et al., 2007), which indicates that, at least in Arabidopsis, MTP8 makes only a minor contribution to Mn tolerance under non-Fe-limiting conditions. Also, the expression patterns of *MTP8* and *MTP11* are very different: whereas *MTP8* is highly expressed only in Fe-deficient roots except for the root tip, *MTP11* expression is most pronounced in this apical area of the root. This indicates that MTP8 and MTP11 have different, non-redundant, and most likely complementary functions and that MTP8 is employed to sequester Mn specifically in those cells that are involved in IRT1-mediated Fe uptake and thus face enhanced Mn influx under Fe deficiency.

MTP8 Is Part of the Fe Acquisition Machinery in Arabidopsis

In Fe-replete conditions, Arabidopsis *MTP8* was expressed at very low levels, while Fe depletion strongly induced its mRNA levels (Fig. 6B). This regulation is mediated by the major transcription factor of Fe acquisition mechanisms in Arabidopsis roots, FIT. Accordingly, *MTP8* expression was strongly enhanced during Fe deficiency in a FIT-dependent manner. This indicated that MTP8 is specifically recruited to detoxify Mn whenever Mn is taken up by IRT1 in superfluous amounts. This function was manifested by determining Mn concentrations in Fe-deficient plants, which were far higher in roots of the wild type than in roots of the mutant (Fig. 9).

Besides Fe, IRT1 not only imports Mn but also other heavy metals, such as Zn, Co, and Ni. Interestingly, the detoxification mechanisms for those IRT1-permeated heavy metals all resemble each other in that the metals are sequestered in the vacuoles of the root cells in which IRT1 is active. Hence, vacuolar loading of excess Zn and Co is mediated by MTP3 (Arrivault et al.,

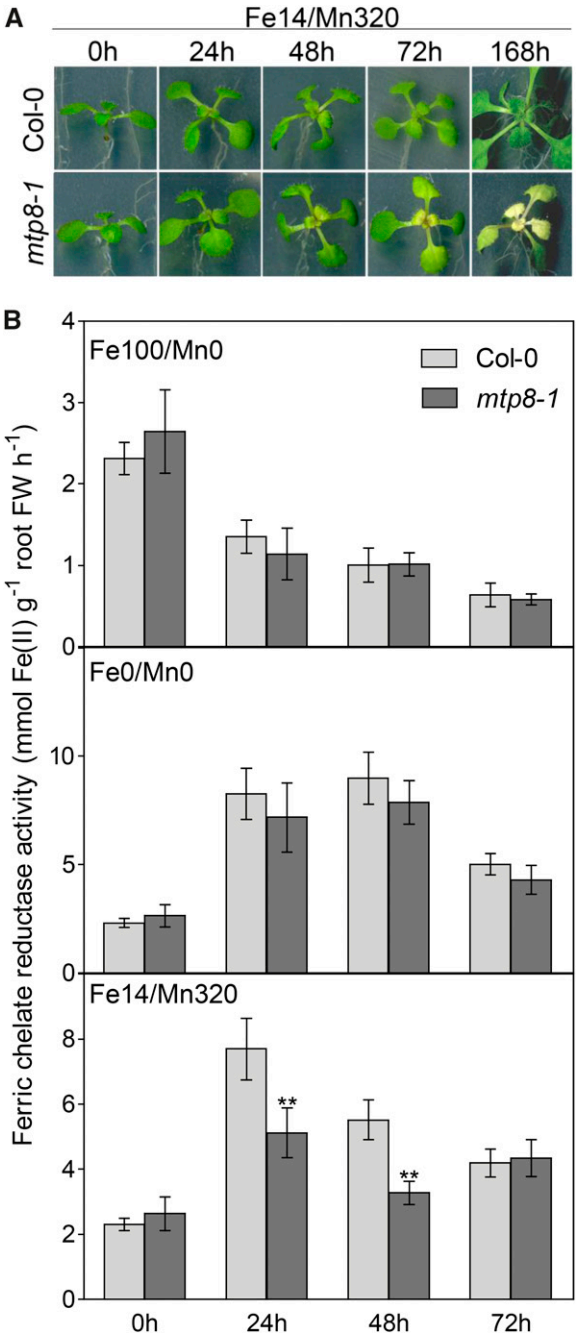

Figure 11. Ferric chelate reduction capacity under Fe deficiency is impaired in *mtp8-1* in the presence of Mn. Seedlings were grown for 11 d on Fe14/Mn0 medium and transferred to Fe100/Mn0, Fe0/Mn0, or Fe14/Mn320 medium. A, Phenotypes of Col-0 and *mtp8-1* mutant plants on Fe14/Mn320 medium. B, Temporal development of ferric chelate reduction capacity under varied Fe/Mn regimes. Three plants for each treatment and genotype were pooled, and the roots were immersed in ferric chelate reductase assay solution on a 12-well plate ($n = 4$). The data point 0 h corresponds to seedlings harvested just before the transfer. The experiment was conducted twice with comparable results. Asterisks indicate that the corresponding mean of the mutant line is significantly different from the mean of the Col-0 line according to Student's *t* test (**, $P < 0.01$). Error bars represent SD. FW, Fresh weight.

2006), excess Ni is sequestered by IREG2 (Schaaf et al., 2006), and MTP8 mediates the vacuolarization of Mn. The purpose of this sequestration of IRT1-permeated heavy metals has so far been seen in the prevention of their movement to the shoot. Our results extend this view and show that the sequestration of an IRT1-permeated heavy metal, in this case Mn, can be essential for an adequate activation of Fe acquisition mechanisms and thus for the tolerance to Fe deficiency-induced chlorosis.

MTP8 expression was also induced by high Mn availability on standard growth medium (Fig. 6, A and C). Although the most straightforward explanation for this may be an Mn-specific regulation of the gene, we found that the induction of *MTP8* is under complete control of the FIT transcription factor, which was confirmed by the loss of *MTP8* expression in Mn-exposed roots of the *fit* mutant (Fig. 6C). This indicated that not Mn, but rather the degree of Mn-induced Fe deficiency, determines *MTP8* transcript levels. Taken together, our data indicate that MTP8 is a component of the Fe acquisition machinery in Arabidopsis required to sustain chlorosis-free growth whenever Mn is present.

MTP8 Allows Chlorosis-Free Growth by Preventing Mn from Inhibiting Fe(III) Reduction

The *mtp8* mutants displayed two distinct phenotypes. First, primary root elongation was reduced on high-Mn medium (Figs. 4 and 8), which is indicative of Mn toxicity (Peiter et al., 2007). Second, *mtp8* mutants displayed severe chlorosis on Mn-containing medium with low Fe availability, by which they were identified in our screen (Fig. 1) and which occurred even before Mn-triggered root growth inhibition set in (Fig. 8). This chlorosis went along with strongly decreased shoot Fe concentrations, confirming that these plants suffered from Fe deficiency-induced chlorosis (Fig. 9). These observations raised the questions of how Mn interferes with Fe nutrition and what role MTP8 plays to counteract the antagonistic Fe-Mn interaction.

One possible explanation for the diminished Fe concentration in *mtp8* shoots might lie in a direct competition of Fe and Mn for xylem loading. Once acquired by the outer root cells, Fe and Mn are translocated radially to the stele to be loaded into the xylem. In the absence of intracellular Mn compartmentalization by MTP8, high Mn uptake from the medium via IRT1 will inevitably increase cytosolic Mn concentrations, which might competitively inhibit Fe export to the xylem, in particular if transport proteins of low specificity are involved. This idea was seemingly supported by the decreased Fe levels in xylem exudate (Supplemental Fig. S4). However, further analyses speak against such a mechanism of Fe-Mn antagonism. A restriction of Fe loading into the xylem would result in an accumulation of Fe in roots, as seen in *man1/frd3* mutants, which are defective in xylem loading of the Fe(III) chelator citrate (Delhaize, 1996; Durrett et al., 2007). However, we never observed an accumulation of Fe in roots of the

mtp8 mutant, neither in elemental analyses nor by Perls's staining of Fe (Fig. 9; Supplemental Fig. S5). Lower Fe concentrations in shoot dry matter were thus caused by an impairment of Fe acquisition rather than Fe translocation.

Alternatively, Mn might suppress the transcriptional response to Fe deficiency, which would then affect the activation of genes involved in Fe mobilization and uptake. We tested this hypothesis but found that the opposite is the case. A number of key transcriptional regulators and Fe acquisition genes were up-regulated when Mn was included in low-Fe medium, and this induction was even more pronounced in the *mtp8* mutant (Fig. 10). Thus, the Fe acquisition machinery was up-regulated in roots of the *mtp8* mutant even to a higher level than in wild-type roots, but it was obviously less efficient in the presence of Mn.

A key step in Fe acquisition lies in the reduction of Fe (III) mediated by the Fe deficiency-induced ferric chelate reductase FRO2. Although the transcript levels of *FRO2* were even higher in *mtp8* than in the wild type, the mutant was unable to realize full ferric chelate reduction capacity in the presence of Mn (Fig. 11). A possible explanation could lie in the low pH optimum of the enzyme, which requires an acidification of the apoplast for maximum activity (Susín et al., 1996). However, we observed that the *mtp8* mutant acidified the growth medium to an even larger extent than the wild type (Supplemental Fig. S6), suggesting that apoplastic pH was not likely a limiting factor for FRO2 activity.

Alternatively, FRO2 protein synthesis or activity may be hypersensitive to Mn in *mtp8* mutants. Evidence for a posttranslational regulation of *FRO2* comes from experiments in which overexpression of the gene did not lead to an increase in ferric chelate reductase activity under Fe sufficiency (Connolly et al., 2003). However, the way by which FRO2 is regulated is not yet clear. FRO2 is modified by Ser phosphorylation at three sites (Zhang et al., 2013) and by Met oxidation at two sites (Engelsberger and Schulze, 2012). It remains to be determined if any of those modifications have a regulatory function that is sensitive to Mn. Also, trafficking of FRO2 to the plasma membrane may be altered by a high Mn load, as is known for the IRT1 protein (Barberon et al., 2014). Therefore, it will be informative to experimentally determine FRO2 localization in the *mtp8* mutant background. A further site of vulnerability to high Mn may lie in the synthesis of the heme cofactor of FRO2. In yeast, heme biosynthesis is affected by Mn due to an inhibition of Fe transport into mitochondria, where heme is produced (Lange et al., 1999). In addition, work on cyanobacteria indicated that Mn inhibits the biosynthesis of tetrapyrrole (Csatorday et al., 1984). A high cytosolic Mn concentration, as expected for the Fe-deficient *mtp8* mutant, may thus lead to a competition of Mn with Fe for heme biosynthesis, which may then be limiting for the synthesis of active FRO2. Future research may particularly consider this specific aspect of heme proteins.

Taken together, the Arabidopsis MTP8 protein occupies a special position among the set of vacuolar transporters that are required to compensate for the low substrate specificity of IRT1. By loading Mn into root vacuoles, MTP8 prevents the inhibition of ferric chelate reduction by Mn and warrants chlorosis-free growth. MTP8 is thus a key player in preventing the antagonistic interference of Mn with Fe nutrition in Arabidopsis. Therefore, the operation of MTP8 is considered crucial for plant survival not only under specific growth conditions on agar but in particular on calcareous soil substrates with elevated pH, where Fe uptake depends on the induction of Fe acquisition mechanisms.

MATERIALS AND METHODS

Plant Lines, Plasmids, and Transformation

All Arabidopsis (*Arabidopsis thaliana*) genotypes used in this study are derived from the Col-0 ecotype. Arabidopsis insertion mutant lines corresponding to 119 different genes (Supplemental Table S1) were obtained from the SALK, GABI, and SAIL collections (Sessions et al., 2002; Alonso et al., 2003; Rosso et al., 2003). Insertions in *mtp8* mutant lines were confirmed by PCR and sequencing of both border regions (Ülker et al., 2008). To construct the pART7:MTP8 plasmid, the *MTP8* cDNA was amplified by RT-PCR from Col-0 RNA using *Xma*I-containing primers (Supplemental Table S2) and cloned into the pART7 vector (Gleave, 1992) downstream of a *CaMV 35S* promoter. To construct the pART7:MTP8:EYFP plasmid, the *MTP8* cDNA without stop codon was amplified from pART7:MTP8 and cloned into the pART7:EYFP vector in frame with *EYFP* (Peiter et al., 2007). For stable transformation of Arabidopsis, an expression cassette (including the *CaMV 35S* promoter and *ocs* terminator) was *Not*I excised from the pART7-derived constructs and inserted into the binary plant transformation vector pBART (Peiter et al., 2007). To construct the pBI101:promoterMTP8:GUS plasmid, the promoter and 5′ untranslated region (−2,046 to −1 bp) of the *MTP8* gene were amplified from Col-0 genomic DNA using *Xma*I-containing primers and cloned into the pBI101 vector upstream of the *uidA* gene (Jefferson et al., 1987). To construct the pGreenII:promoterMTP8:MTP8:EYFP plasmid, a *promoterMTP8* fragment was excised from pBI101:promoterMTP8:GUS using *Sma*I and cloned into the pGreenII plasmid (Hellens et al., 2000). Subsequently, an *MTP8:EYFP:ocs* fragment was excised from pART7:MTP8:EYFP by using *Not*I and *Eco*RV and cloned into the pGreenII:promoterMTP8 plasmid downstream of the *MTP8* promoter.

Stable transformation of Arabidopsis with *Agrobacterium tumefaciens* GV3101 was carried out by the floral dip method (Clough and Bent, 1998). Transformants containing pBART and pGreenII constructs were selected by spraying with BASTA, and those containing pBI101 constructs were selected on kanamycin-containing plates. Transient transformation of Arabidopsis mesophyll protoplasts was performed as described previously (Peiter et al., 2005b).

Plant Growth Conditions, Media, and Mutant Screening

For sterile cultivation on agar plates, seeds were surface sterilized in 70% (v/v) ethanol and 0.05% (v/v) Triton X-100. Seeds were sown at a distance of approximately 1 cm from each other and stratified for 2 d at 4°C in darkness. Plates were oriented vertically in a growth cabinet (Percival Scientific) set to 22°C day and 19°C night temperatures and a 10-h light period with a light intensity of 120 μmol photons m^{-2} s^{-1}.

In order to develop an agar medium with low Fe availability, one-half-strength MS medium without Fe and Mn (Duchefa Biochemie), containing 15 g L^{-1} agar (Difco) and 5 g L^{-1} Suc, was used as a basal medium. To decrease the Fe availability, the medium was buffered with 10 mM MES adjusted to pH 6.7 with NaOH. Fe was added to the medium as NaFe(III)-EDTA and Mn as $MnCl_2$ in the concentrations indicated. In experiments where plants were cultivated on standard one-half-strength MS medium, the pH of the medium was buffered to 5.5 with 2.5 mM MES-NaOH.

To observe growth on soil, seeds were sown onto standard potting soil (Substrat 1; Klasmann-Deilmann). In order to increase pH to limit Fe availability, the soil was supplemented with 20 g kg^{-1} $CaCO_3$ and 12 g kg^{-1} $NaHCO_3$. After 13 d of preculture, seedlings were watered for 6 d with 160 μM $MnCl_2$ and

photographed thereafter. To measure soil pH, 2.5 g of soil was suspended in 25 mL of a 10 mM $CaCl_2$ solution. After filtration, pH of the solution was determined by a pH meter.

Yeast Strains, Plasmids, Transformation, and Growth Methods

The *Saccharomyces cerevisiae* deletion mutants Y04534 (*pmr1Δ*), Y04069 (*ycf1Δ*), Y00829 (*zrc1Δ*), Y01613 (*cot1Δ*), and Y04533 (*cup2Δ*) and their parental strain BY4741 were obtained from the Euroscarf collection (Winzeler et al., 1999). To construct the pFL61:MTP8 plasmid, the *MTP8* cDNA was amplified from pART7:MTP8 using *Not*I-containing primers and cloned into the pFL61 yeast expression vector (Minet et al., 1992) downstream of a *PHOSPHOGLYCERATE KINASE* (*PGK*) promoter. Yeast transformation was carried out according to Elble (1992). Transformants were selected on synthetic complete plates lacking the appropriate selective markers (Sherman, 2002). Yeast drop assays were performed as described previously (Peiter et al., 2005a).

^{54}Mn Uptake Experiments

Microsomal membranes were isolated from log-phase cultures of *pmr1Δ* pFL61 and *pmr1Δ* pFL61-MTP8 yeast strains grown in synthetic complete medium according to Ueoka-Nakanishi et al. (2000), and uptake assays were performed as described previously (Peiter et al., 2007) with some modifications. $MnCl_2$, labeled with $^{54}Mn^{2+}$ (2,083 MBq mg^{-1}; PerkinElmer Life Science), was added to yeast vesicles incubated in uptake buffer {5 mM BTP/MES (pH 7.5), 300 mM sorbitol, 25 mM KCl, and 5 mM $MgCl_2$} with or without 1 mM ATP to a final concentration of 100 μM Mn^{2+}. Aliquots were vacuum filtered through 25-mm cellulose nitrate membrane filters (0.45 μM; Whatman) at the specified time points. Filters were washed two times with 5 mL of ice-cold washing buffer {5 mM BTP/MES (pH 7.5), 300 mM sorbitol, 25 mM KCl, and 1 mM $MnSO_4$}, and $^{54}Mn^{2+}$ activity trapped on the filter was determined by using a liquid scintillation counter (TriCarb; PerkinElmer Life Science). Values of samples incubated without ATP were subtracted from the corresponding values of samples with ATP to correct for unspecific adsorption.

Elemental Analyses

Roots and shoots of plants were separated, rinsed with deionized water, and dried at 65°C for 1 week. The dried shoots and roots were weighed into polytetrafluoroethylene (PTFE) digestion tubes and digested in HNO_3 under pressure using a microwave digester (UltraCLAVE IV; MLS). Elemental analysis was undertaken using ICP-OES (iCAP 6500 dual optical emission spectrometer; Thermo Fisher Scientific).

For elemental analysis of intact vacuoles, Arabidopsis plants grown for 7 weeks in nutrient solution according to Peiter et al. (2007) were transferred to the same solution containing 240 μM $MnSO_4$ and cultivated further for 7 d. Root protoplasts were isolated as described by Bargmann and Birnbaum (2010). Intact vacuoles of those protoplasts were isolated according to Shimaoka et al. (2004) and digested in perfluoroalkoxy alkane (PFA) vessels with 1.5 mL of HNO_3 (65%) and 0.6 mL of H_2O_2 (30%) for 15 min at 180°C (MARS 5 Xpress; CEM). The digestate was analyzed by high-resolution ICP-MS (ELEMENT 2; Thermo Fisher Scientific). Prior to digestion, the number of vacuoles was determined using a Fuchs-Rosenthal hemacytometer (Marienfeld).

Xylem Exudate Analysis

Wild-type and mutant plants were grown for 5 weeks on aerated liquid one-half-strength MS medium, transferred to liquid Fe28/Mn40 medium, and cultivated further for 7 d. For the collection of xylem exudate, rosettes were removed by sharp razor blades, and silicon tubes with a diameter of 1 mm were connected to the hypocotyls. After discarding the first 5 μL, exudates were collected into microtubes for 2 h, and metal concentrations in exudates were analyzed by ICP-MS.

Perls's Staining

Whole Arabidopsis roots were incubated in Perls's reagent (equal amounts of solutions of 4% [v/v] HCl and 4% [w/v] potassium ferrocyanide) for 45 min. Roots were washed in distilled water to stop the reaction and observed with a light microscope.

Histochemical GUS Analyses

Samples were incubated at 37°C in a GUS reaction buffer containing 0.4 mg mL^{-1} 5-bromo-4-chloro-3-indolyl-β-D-glucuronide, 50 mM sodium phosphate (pH 7.2), and 0.5 mM ferrocyanide. Five *PromoterMTP8:GUS* lines were examined and showed the same staining patterns under standard growth conditions. Of those lines, two were analyzed in more detail. To this end, shoot samples were cleared and mounted as described by Malamy and Benfey (1997). For microscopic observations of root cross sections, samples were fixed in 2% formaldehyde and 2% glutaraldehyde in 50 mM cacodylate buffer (pH 7.2), dehydrated in an ethanol series (30%, 40%, ..., 100%), and embedded in Spurr's resin. Five-micrometer cross sections of stained roots were obtained by cutting the fixed and resin-embedded samples using a microtome (Ultracut; Leica) and observed with a light microscope (Axioskop; Carl Zeiss).

Chlorophyll Measurements

Chlorophyll concentrations were determined by extracting shoot samples with spectrophotometric grade *N*,*N*′-dimethyl formamide (Sigma-Aldrich) at 4°C for 48 h. The absorbance at 647 and 664 nm was measured in extracts according to Porra et al. (1989).

Imaging of Plants and Protoplasts

Images of agar-grown plants were captured using a flatbed scanner (Expression 10000XL; Epson) at a resolution of 300 dots per inch. Protoplasts expressing *MTP8:EYFP* were observed by confocal laser scanning microscopy using an LSM 510 Meta head based on an Axiovert 200M microscope (Zeiss). Images were obtained in λ mode as described by Peiter et al. (2007).

Quantitative RT-PCR

For the expression analyses shown in Figures 5A and 6A, RNA was isolated from N_2-ground plant material using an RNeasy plant mini kit (Qiagen) with on-column DNase treatment according to the manufacturer's instructions. cDNA was prepared from 1 μg of RNA using random hexamer primers and SuperScript II reverse transcriptase (Life Technologies) according to the manufacturer's protocol. Quantitative real-time PCR was carried out on a Mastercycler ep realplex^4 S (Eppendorf) using the POWER SYBR Green PCR Mastermix (Applied Biosystems). Expression levels of *MTP8*, *IRT1*, *FRO2*, and *FIT1* were determined by relative quantification against a standard curve derived from a cDNA dilution series. *MTP8* expression was normalized against *ACTIN2* as a constitutively expressed control.

For Figures 6, B and C, and 10, RNA was isolated using a modified version of the single-step method (Chomczynski and Sacchi, 1987). For RT of RNA into cDNA, the RevertAid First Strand cDNA Synthesis Kit (Fermentas), oligo(dT) primers, and RNA samples treated with RQ1 RNase-free DNase (Promega) were used. Gene expression was analyzed by quantitative real-time PCR using a Mastercycler ep realplex (Eppendorf) and iQ SYBR Green Supermix (Bio-Rad). Relative expression was calculated according to Pfaffl (2001) and normalized against *UBQ2* as a constitutively expressed control.

Ferric Chelate Reductase and Rhizosphere Acidification Assays

Seedlings were cultivated on Fe14/Mn0 for 11 d, and similar-sized ones were transferred to Fe100/Mn0, Fe0/Mn0, or Fe14/Mn320. After 0, 24, 48, and 72 h, seedlings were assayed for ferric chelate reductase activity as described by Waters et al. (2006). Three to five plants were pooled, and roots were placed into a 2-mL buffer solution containing 0.2 mM $CaSO_4$, 5 mM MES (pH 5.5), 0.2 mM ferrozine, and 0.1 mM Fe-EDTA on a 24-well plate. The reaction was allowed to continue for 1 to 2 h. Seedlings were then removed from the solution, and roots were excised, quickly dried on tissue paper, and weighed. Absorbance of the solutions at 562 nm was measured using a UV-VIS light spectrophotometer (Uvikon XL; Biotek).

For the rhizosphere acidification assay, plants were cultivated as described above for the ferric chelate reductase activity assay. The assay was conducted as described previously (Yi and Guerinot, 1996). In brief, seedlings that had been cultivated for 24, 48, or 72 h on Fe100/Mn0, Fe0/Mn0, or Fe14/Mn320 were transferred to a 1% agar plate containing 0.006% Bromocresol Purple and 0.2 mM $CaSO_4$ (adjusted to pH 6.5 with NaOH) and incubated in the growth chamber for 24 h.

Supplemental Data

The following supplemental materials are available.

Supplemental Figure S1. Effect of Fe concentration on the growth of mutants on high-pH medium.

Supplemental Figure S2. Genotypical analysis of *MTP8* T-DNA mutant lines.

Supplemental Figure S3. Elongation of *mtp8-1* primary roots is hypersensitive to high Mn concentrations.

Supplemental Figure S4. Fe translocation in the xylem stream is decreased in the *mtp8-1* mutant.

Supplemental Figure S5. Roots of the *mtp8-1* mutant do not accumulate more iron than wild-type plants.

Supplemental Figure S6. Rhizosphere acidification under Fe deficiency is enhanced in *mtp8-1* in the presence of Mn.

Supplemental Table S1. T-DNA mutants screened for sensitivity to low Fe availability.

Supplemental Table S2. Primers used in this study.

ACKNOWLEDGMENTS

We thank Kristin Peter (Martin Luther University Halle-Wittenberg), Michael Melzer, and Susanne Reiner (both IPK Gatersleben) for excellent technical assistance and Sven-Eric Behrens (Institute for Biochemistry and Biotechnology, Martin Luther University Halle-Wittenberg) for granting access to the confocal laser scanning microscope.

Received August 3, 2015; accepted December 6, 2015; published December 14, 2015.

LITERATURE CITED

Alonso JM, Stepanova AN, Leisse TJ, Kim CJ, Chen H, Shinn P, Stevenson DK, Zimmerman J, Barajas P, Cheuk R, et al (2003) Genome-wide insertional mutagenesis of *Arabidopsis thaliana*. Science **301:** 653–657

Antebi A, Fink GR (1992) The yeast Ca^{2+}-ATPase homologue, PMR1, is required for normal Golgi function and localizes in a novel Golgi-like distribution. Mol Biol Cell **3:** 633–654

Arrivault S, Senger T, Krämer U (2006) The Arabidopsis metal tolerance protein AtMTP3 maintains metal homeostasis by mediating Zn exclusion from the shoot under Fe deficiency and Zn oversupply. Plant J **46:** 861–879

Barberon M, Dubeaux G, Kolb C, Isono E, Zelazny E, Vert G (2014) Polarization of IRON-REGULATED TRANSPORTER 1 (IRT1) to the plant-soil interface plays crucial role in metal homeostasis. Proc Natl Acad Sci USA **111:** 8293–8298

Barberon M, Zelazny E, Robert S, Conéjéro G, Curie C, Friml J, Vert G (2011) Monoubiquitin-dependent endocytosis of the iron-regulated transporter 1 (IRT1) transporter controls iron uptake in plants. Proc Natl Acad Sci USA **108:** E450–E458

Bargmann BOR, Birnbaum KD (2010) Fluorescence activated cell sorting of plant protoplasts. J Vis Exp **36:** 1673

Buckhout TJ, Yang TJW, Schmidt W (2009) Early iron-deficiency-induced transcriptional changes in *Arabidopsis* roots as revealed by microarray analyses. BMC Genomics **10:** 147

Chen Z, Fujii Y, Yamaji N, Masuda S, Takemoto Y, Kamiya T, Yusuyin Y, Iwasaki K, Kato S, Maeshima M, et al (2013) Mn tolerance in rice is mediated by MTP8.1, a member of the cation diffusion facilitator family. J Exp Bot **64:** 4375–4387

Chomczynski P, Sacchi N (1987) Single-step method of RNA isolation by acid guanidinium thiocyanate-phenol-chloroform extraction. Anal Biochem **162:** 156–159

Clough SJ, Bent AF (1998) Floral dip: a simplified method for *Agrobacterium*-mediated transformation of *Arabidopsis thaliana*. Plant J **16:** 735–743

Colangelo EP, Guerinot ML (2004) The essential basic helix-loop-helix protein FIT1 is required for the iron deficiency response. Plant Cell **16:** 3400–3412

Connolly EL, Campbell NH, Grotz N, Prichard CL, Guerinot ML (2003) Overexpression of the FRO2 ferric chelate reductase confers tolerance to growth on low iron and uncovers posttranscriptional control. Plant Physiol **133:** 1102–1110

Csatorday K, Gombos Z, Szalontai B (1984) Mn^{2+} and Co^{2+} toxicity in chlorophyll biosynthesis. Proc Natl Acad Sci USA **81:** 476–478

Delhaize E (1996) A metal-accumulator mutant of *Arabidopsis thaliana*. Plant Physiol **111:** 849–855

Delhaize E, Gruber BD, Pittman JK, White RG, Leung H, Miao Y, Jiang L, Ryan PR, Richardson AE (2007) A role for the *AtMTP11* gene of Arabidopsis in manganese transport and tolerance. Plant J **51:** 198–210

Delhaize E, Kataoka T, Hebb DM, White RG, Ryan PR (2003) Genes encoding proteins of the cation diffusion facilitator family that confer manganese tolerance. Plant Cell **15:** 1131–1142

Durrett TP, Gassmann W, Rogers EE (2007) The FRD3-mediated efflux of citrate into the root vasculature is necessary for efficient iron translocation. Plant Physiol **144:** 197–205

Eide D, Broderius M, Fett J, Guerinot ML (1996) A novel iron-regulated metal transporter from plants identified by functional expression in yeast. Proc Natl Acad Sci USA **93:** 5624–5628

Elble R (1992) A simple and efficient procedure for transformation of yeasts. Biotechniques **13:** 18–20

Engelsberger WR, Schulze WX (2012) Nitrate and ammonium lead to distinct global dynamic phosphorylation patterns when resupplied to nitrogen-starved Arabidopsis seedlings. Plant J **69:** 978–995

Erbasol I, Bozdag GO, Koc A, Pedas P, Karakaya HC (2013) Characterization of two genes encoding metal tolerance proteins from *Beta vulgaris* subspecies *maritima* that confers manganese tolerance in yeast. Biometals **26:** 795–804

Giehl RFH, Meda AR, von Wirén N (2009) Moving up, down, and everywhere: signaling of micronutrients in plants. Curr Opin Plant Biol **12:** 320–327

Gile PL (1916) Chlorosis of pineapples induced by manganese and carbonate of lime. Science **44:** 855–857

Gleave AP (1992) A versatile binary vector system with a T-DNA organisational structure conducive to efficient integration of cloned DNA into the plant genome. Plant Mol Biol **20:** 1203–1207

Gruber BD, Giehl RFH, Friedel S, von Wirén N (2013) Plasticity of the Arabidopsis root system under nutrient deficiencies. Plant Physiol **163:** 161–179

Gustin JL, Zanis MJ, Salt DE (2011) Structure and evolution of the plant cation diffusion facilitator family of ion transporters. BMC Evol Biol **11:** 76

Hellens RP, Edwards EA, Leyland NR, Bean S, Mullineaux PM (2000) pGreen: a versatile and flexible binary Ti vector for *Agrobacterium*-mediated plant transformation. Plant Mol Biol **42:** 819–832

Hewitt EJ (1948) Relation of manganese and some other metals to the iron status of plants. Nature **161:** 489–490

Ivanov R, Brumbarova T, Blum A, Jantke AM, Fink-Straube C, Bauer P (2014) SORTING NEXIN1 is required for modulating the trafficking and stability of the *Arabidopsis* IRON-REGULATED TRANSPORTER1. Plant Cell **26:** 1294–1307

Jakoby M, Wang H-Y, Reidt W, Weisshaar B, Bauer P (2004) *FRU* (*BHLH029*) is required for induction of iron mobilization genes in *Arabidopsis thaliana*. FEBS Lett **577:** 528–534

Jefferson RA, Kavanagh TA, Bevan MW (1987) GUS fusions: beta-glucuronidase as a sensitive and versatile gene fusion marker in higher plants. EMBO J **6:** 3901–3907

Kobayashi T, Nishizawa NK (2012) Iron uptake, translocation, and regulation in higher plants. Annu Rev Plant Biol **63:** 131–152

Korshunova YO, Eide D, Clark WG, Guerinot ML, Pakrasi HB (1999) The IRT1 protein from *Arabidopsis thaliana* is a metal transporter with a broad substrate range. Plant Mol Biol **40:** 37–44

Lange H, Kispal G, Lill R (1999) Mechanism of iron transport to the site of heme synthesis inside yeast mitochondria. J Biol Chem **274:** 18989–18996

Lindner RC, Harley CP (1944) Nutrient interrelations in lime-induced chlorosis. Plant Physiol **19:** 420–439

Lindsay WL, Schwab AP (1982) The chemistry of iron in soils and its availability to plants. J Plant Nutr **5:** 821–840

Long TA, Tsukagoshi H, Busch W, Lahner B, Salt DE, Benfey PN (2010) The bHLH transcription factor POPEYE regulates response to iron deficiency in *Arabidopsis* roots. Plant Cell **22:** 2219–2236

Malamy JE, Benfey PN (1997) Organization and cell differentiation in lateral roots of *Arabidopsis thaliana*. Development **124:** 33–44

Marschner P (2012) Marschner's Mineral Nutrition of Higher Plants. Elsevier, Amsterdam

Migocka M, Papierniak A, Maciaszczyk-Dziubińska E, Poździk P, Posyniak E, Garbiec A, Filleur S (2014) Cucumber metal transport protein MTP8 confers increased tolerance to manganese when expressed in yeast and *Arabidopsis thaliana*. J Exp Bot **65:** 5367–5384

Minet M, Dufour M-E, Lacroute F (1992) Complementation of *Saccharomyces cerevisiae* auxotrophic mutants by *Arabidopsis thaliana* cDNAs. Plant J **2:** 417–422

Montanini B, Blaudez D, Jeandroz S, Sanders D, Chalot M (2007) Phylogenetic and functional analysis of the Cation Diffusion Facilitator (CDF) family: improved signature and prediction of substrate specificity. BMC Genomics **8:** 107

Murashige T, Skoog F (1962) A revised medium for rapid growth and bio assays with tobacco tissue cultures. Physiol Plant **15:** 473–497

Pedas P, Schiller Stokholm M, Hegelund JN, Ladegård AH, Schjoerring JK, Husted S (2014) Golgi localized barley *MTP8* proteins facilitate Mn transport. PLoS ONE **9:** e113759

Peiter E (2014) Mineral deficiencies. *In* G-J Krauss, DH Nies, eds, Ecological Biochemistry. Wiley-VCH, Weinheim, Germany, pp 209–222

Peiter E, Fischer M, Sidaway K, Roberts SK, Sanders D (2005a) The *Saccharomyces cerevisiae* Ca^{2+} channel Cch1pMid1p is essential for tolerance to cold stress and iron toxicity. FEBS Lett **579:** 5697–5703

Peiter E, Maathuis FJM, Mills LN, Knight H, Pelloux J, Hetherington AM, Sanders D (2005b) The vacuolar Ca^{2+}-activated channel TPC1 regulates germination and stomatal movement. Nature **434:** 404–408

Peiter E, Montanini B, Gobert A, Pedas P, Husted S, Maathuis FJM, Blaudez D, Chalot M, Sanders D (2007) A secretory pathway-localized cation diffusion facilitator confers plant manganese tolerance. Proc Natl Acad Sci USA **104:** 8532–8537

Pfaffl MW (2001) A new mathematical model for relative quantification in real-time RT-PCR. Nucleic Acids Res **29:** e45

Porra RJ, Thompson WA, Kriedemann PE (1989) Determination of accurate extinction coefficients and simultaneous equations for assaying chlorophylls *a* and *b* extracted with four different solvents: verification of the concentration of chlorophyll standards by atomic absorption spectroscopy. Biochim Biophys Acta **975:** 384–394

Ricachenevsky FK, Menguer PK, Sperotto RA, Williams LE, Fett JP (2013) Roles of plant metal tolerance proteins (MTP) in metal storage and potential use in biofortification strategies. Front Plant Sci **4:** 144

Robinson NJ, Procter CM, Connolly EL, Guerinot ML (1999) A ferric-chelate reductase for iron uptake from soils. Nature **397:** 694–697

Rosso MG, Li Y, Strizhov N, Reiss B, Dekker K, Weisshaar B (2003) An *Arabidopsis thaliana* T-DNA mutagenized population (GABI-Kat) for flanking sequence tag-based reverse genetics. Plant Mol Biol **53:** 247–259

Santi S, Schmidt W (2009) Dissecting iron deficiency-induced proton extrusion in Arabidopsis roots. New Phytol **183:** 1072–1084

Schaaf G, Honsbein A, Meda AR, Kirchner S, Wipf D, von Wirén N (2006) AtIREG2 encodes a tonoplast transport protein involved in iron-dependent nickel detoxification in *Arabidopsis thaliana* roots. J Biol Chem **281:** 25532–25540

Schmid NB, Giehl RFH, Döll S, Mock HP, Strehmel N, Scheel D, Kong X, Hider RC, von Wirén N (2014) Feruloyl-CoA 6′-hydroxylase1-dependent coumarins mediate iron acquisition from alkaline substrates in Arabidopsis. Plant Physiol **164:** 160–172

Sessions A, Burke E, Presting G, Aux G, McElver J, Patton D, Dietrich B, Ho P, Bacwaden J, Ko C, et al (2002) A high-throughput Arabidopsis reverse genetics system. Plant Cell **14:** 2985–2994

Sherman F (2002) Getting started with yeast. Methods Enzymol **350:** 3–41

Shimaoka T, Ohnishi M, Sazuka T, Mitsuhashi N, Hara-Nishimura I, Shimazaki K-I, Maeshima M, Yokota A, Tomizawa K-I, Mimura T (2004) Isolation of intact vacuoles and proteomic analysis of tonoplast from suspension-cultured cells of *Arabidopsis thaliana*. Plant Cell Physiol **45:** 672–683

Shin L-J, Lo J-C, Chen G-H, Callis J, Fu H, Yeh K-C (2013) IRT1 DEGRADATION FACTOR1, a ring E3 ubiquitin ligase, regulates the degradation of IRON-REGULATED TRANSPORTER1 in *Arabidopsis*. Plant Cell **25:** 3039–3051

Sideris CP, Young HY (1949) Growth and chemical composition of *Ananas comosus* (L.) Merr., in solution cultures with different iron-manganese ratios. Plant Physiol **24:** 416–440

Somers II, Shive JW (1942) The iron-manganese relation in plant metabolism. Plant Physiol **17:** 582–602

Susín S, Abadía A, González-Reyes JA, Lucena JJ, Abadía J (1996) The pH requirement for in vivo activity of the iron deficiency-induced "turbo" ferric chelate reductase: a comparison of the iron-deficiency-induced iron reductase activities of intact plants and isolated plasma membrane fractions in sugar beet. Plant Physiol **110:** 111–123

Twyman ES (1946) The iron-manganese balance and its effect on the growth and development of plants. New Phytol **45:** 18–24

Ueoka-Nakanishi H, Tsuchiya T, Sasaki M, Nakanishi Y, Cunningham KW, Maeshima M (2000) Functional expression of mung bean Ca^{2+}/H^{+} antiporter in yeast and its intracellular localization in the hypocotyl and tobacco cells. Eur J Biochem **267:** 3090–3098

Ülker B, Peiter E, Dixon DP, Moffat C, Capper R, Bouché N, Edwards R, Sanders D, Knight H, Knight MR (2008) Getting the most out of publicly available T-DNA insertion lines. Plant J **56:** 665–677

Vert G, Grotz N, Dédaldéchamp F, Gaymard F, Guerinot ML, Briat J-F, Curie C (2002) IRT1, an Arabidopsis transporter essential for iron uptake from the soil and for plant growth. Plant Cell **14:** 1223–1233

Waters BM, Chu H-H, DiDonato RJ, Roberts LA, Eisley RB, Lahner B, Salt DE, Walker EL (2006) Mutations in Arabidopsis *Yellow Strip-Like1* and *Yellow Stripe-Like3* reveal their roles in metal ion homeostasis and loading of metal ions in seeds. Plant Physiol **141:** 1446–1458

Winzeler EA, Shoemaker DD, Astromoff A, Liang H, Anderson K, Andre B, Bangham R, Benito R, Boeke JD, Bussey H, et al (1999) Functional characterization of the *S. cerevisiae* genome by gene deletion and parallel analysis. Science **285:** 901–906

Yi Y, Guerinot ML (1996) Genetic evidence that induction of root Fe(III) chelate reductase activity is necessary for iron uptake under iron deficiency. Plant J **10:** 835–844

Zhang H, Zhou H, Berke L, Heck AJR, Mohammed S, Scheres B, Menke FLH (2013) Quantitative phosphoproteomics after auxin-stimulated lateral root induction identifies an SNX1 protein phosphorylation site required for growth. Mol Cell Proteomics **12:** 1158–1169